Biogeographical distribution of *Rimicaris exoculata* resident gut epibiont communities along the Mid-Atlantic Ridge hydrothermal vent sites

Durand Lucile [1], Roumagnac Marie [1], Cueff-Gauchard Valerie [1], Jan Cyrielle [2], Guri Mathieu [3], Tessier Claire [1], Haond Marine [1], Crassous Philippe [4], Zbinden Magali [5], Arnaud-Haond Sophie [4], Cambon-Bonavita Marie-Anne [1, *]

[1] Ifremer, Centre de Brest, Laboratoire de Microbiologie des Environnements Extremes, REM/EEP/LM2E, UMR 6197 Ifremer-CNRS-UBO, BP 70, 29280 Plouzane, France,
[2] Université de Brest, Laboratoire de Microbiologie des Environnements Extremes, UMR 6197 Ifremer-CNRS-UBO, Technopole Iroise, 4 place Nicolas Copernic, 29280 Plouzane, France
[3] CNRS, Laboratoire de Microbiologie des Environnements Extremes, UMR 6197 Ifremer-CNRS-UBO, Technopole Iroise, 4 place Nicolas Copernic, 29280 Plouzane, France
[4] Ifremer, Centre de Brest, Laboratoire Environnements Profonds, REM/EEP/LEP, 29280 Plouzane, France
[5] UMR CNRS 7208 BOREA, Equipe aux Milieux Extremes, Universite Pierre et Marie Curie Paris VI, 7 Quai Saint Bernard, 75252 Paris cedex 05, France

* Corresponding author : Marie-Anne Cambon-Bonavita, Tel: +33-298224756; Fax: +33-298224757 ;
email address : marie.anne.cambon@ifremer.fr

Abstract :

Rimicaris exoculata is a deep-sea hydrothermal vent shrimp which enlarged gill chamber houses a complex trophic epibiotic community. Its gut harbours an autochthonous and distinct microbial community. This species dominates hydrothermal ecosystems megafauna along the Mid-Atlantic Ridge, regardless of contrasted geochemical conditions prevailing in them. Here, the resident gut epibiont community at four contrasted hydrothermal vent sites (Rainbow/TAG/Logatchev/Ashadze) was analysed and compiled with previous data to evaluate the possible influence of site location, using 16S rRNA surveys and microscopic observations (TEM, SEM and FISH analyses). Filamentous epibionts inserted between the epithelial cells microvilli were observed on all examined samples. Results confirmed resident gut community affiliation to *Deferribacteres*, *Mollicutes*, *Epsilonproteobacteria* and to a lesser extent *Gammaproteobacteria* lineages. Still a single *Deferribacteres* phylotype was retrieved at all sites. Four *Mollicutes*-related OTUs were distinguished, one being only identified on Rainbow specimens. The topology of ribotypes median-joining networks illustrated a community diversification possibly following demographic expansions, suggesting a more ancient evolutionary history and/or a larger effective population size at Rainbow. Finally, the gill chamber community distribution was also analysed through ribotypes networks based on sequences from *R. exoculata* collected at Rainbow/Snake Pit/TAG/Logatchev/Ashadze sites. Results allow refining hypotheses on the epibiont role and transmission pathways.

Keywords : epibiont, extreme environments, network analyses, phylogeography

Introduction

Deep-sea hydrothermal ecosystems described all along mid-ocean ridges are sustained by microbial chemosynthesis in place of photosynthesis predominating in the photic zone. On the Mid-Atlantic Ridge (MAR), hydrothermal vents are known from the North of the Azores Triple Junction to the South MAR site (Fig.1a). These hydrothermal vents are characterized by contrasted geochemical conditions (Charlou *et al.*, 2010; Kelley *et al.*, 2001) depending on the crust rock nature crossed by the hydrothermal fluids. Basalt-hosted sites (such as Snake Pit, Lucky Strike and TAG) expel fluids reaching temperatures up to 300°C, enriched in sulphides and silica but relatively depleted in methane and hydrogen. In contrast, ultramafic-hosted sites (such as Rainbow, Logatchev, South MAR and the recently studied Ashadze sites) expel fluids influenced by mantle rocks, relatively poor in sulphides but enriched in methane, hydrogen, carbon monoxide, iron, calcium, abiotic long-chain hydrocarbons (Charlou *et al.*, 2010). But each site, since they were first sampled, shows that the fluids composition is stable, which is particularly true for the Rainbow site indicating probably a unique origin (Charlou et al., 2010).

Hydrothermal vents harbor a dense and endemic fauna which has developed strategies to colonize new sites and circumvent spatially contrasted geochemical conditions. Usually, faunal assemblages are distributed in concentric areas around vent fluid emissions (Desbruyères *et al.*, 2001). At MAR locations, anemones and gastropods are located at low temperatures (2-5°C) circled by bivalves and crustaceans (from 5 to 30°C).The caridean shrimp *Rimicaris exoculata* (Williams & Rona, 1986) lives in the areas of upper temperature, in dense aggregates close to the active chimney walls (Komaï & Segonzac, 2008 for review; Schmidt *et al.*, 2008; Ravaux *et al.*, 2009). This species is endemic of MAR hydrothermal vent sites, both basaltic- and ultramafic-hosted systems. The genus is also retrieved at the Central Indian Ridge and in the Mid-

Cayman Spreading Centre (Watabe & Hashimoto, 2002; Nye *et al.*, 2012). The aggregates are highly active and dense whatever the site considered, except at Ashadze where only few adults were observed (Fig.S1b). At this site megafauna was neither much diverse nor abundant, mainly composed of anemones and chaetopterid polychaetes (Fabri *et al.*, 2011).

60   Two microbial epibiont colonization areas were described associated with *R. exoculata*. The first one located in its gill chamber (Van Dover *et al.*, 1988; Casanova *et al.*, 1993; Segonzac *et al.*, 1993; Polz & Cavanaugh, 1995; Gebruk *et al.*, 2000; Zbinden *et al.*, 2004, 2008; Corbari *et al.*, 2008a, 2008b; Petersen *et al.*, 2010; Hügler *et al.*, 2011; Guri *et al.*, 2012). It is a complex but stable epibiont community, mainly affiliated to *Proteobacteria* lineages (Jan *et al.*, 2014) and composed of at least sulphur-, iron-, methane- and hydrogen-oxidizers at the Rainbow ultramafic-hosted site (Zbinden *et al.*, 2008; Guri *et al.*, 2012, Jan *et al.*, 2014). This epibiont community is implied in the shrimp nutrition (Ponsard *et al.*,

65   2013). This relative diversity could explain that this shrimp fit well with contrasted geochemical conditions. While in direct contact with the outer medium, this community is stable at the genus level whatever the site and sampling period. At the ribotype level this community was reported as site-dependant, and could thus be acquired from the environment (horizontal transmission) at each generation and after each moult (Petersen *et al.*, 2010) to improve fitness. The second one, located in the gut, is characterized by four main phyla: *Deferribacteres*, *Mollicutes*, *Epsilonproteobacteria* and to a lesser extent *Gammaproteobacteria* (Polz *et al.*, 1998; Zbinden & Cambon-Bonavita, 2003; Durand *et al.*, 2010).

70   Those lineages, retrieved after each sampling, are also still present after a 72 hours starvation experiment leading to completely empty the gut. They were then called resident epibiont (Durand *et al.*, 2010). The gut epibiont transmission via parents (vertical) or via the environment (horizontal) is still debated. Among those phyla, free living *Epsilon-* and *Gammaproteobacteria* are commonly identified in hydrothermal ecosystems but none of the *Deferribacteres* species affiliated to *R. exoculata* gut epibionts (close to *Geovibrio* and *Mucispirillum*) have ever

been reported (López-García *et al.*, 2003; Voordeckers *et al.*, 2008; Brazelton *et al.*, 2010; Flores *et al.*, 2011; Guri *et al.*, 2012). For Mollicutes,

75   only one recent study reports a single related clone sequence in environmental samples from hydrothermal vents collected above mussels and

Rimicaris exoculata aggregates (Hügler *et al.*, 2010) but this finding was not confirmed through pyrosequencing analysis (Flores *et al.*, 2011).

The role of these lineages is still poorly understood as they seem not highly implied in the host nutrition (Ponsard et *al.*, 2013).

The first aim of this study was to confirm the four lineages resident gut epibiosis at different locations, using both microscopic and molecular

approaches based on DNA and RNA ("present" and "active" microbial community respectively). Secondly, a multi-site survey was done to test

80   the hypothesis of site-influence on the resident epibiont lineages to attempt to trace back their origin. For this purpose, the resident gut epibiont

community associated with *R. exoculata* from four MAR hydrothermal vent sites TAG, Rainbow, Logatchev and Ashadze, was analysed with

compiled data from previous studies on communities associated with the gut (Rainbow and TAG) and with the gill chamber at Rainbow, Snake

Pit and South MAR (Tab. 2, Fig.1a).

Materials and methods

85   ***Sample collection***

Samples for the gut epibionts present study were collected at four MAR hydrothermal vent sites (Fig.1a) during successive cruises: TAG, 26°8'N-44°50'W, 3650 m depth (EXOMAR 2005); Rainbow, 36°14'N-33°54'W, 2320 m depth (ATOS 2001, EXOMAR 2005, MoMARDREAM-Naut 2007, MoMAR08 2008); Logatchev, 14°45'N-44°58'W, 3000 m depth and Ashadze, 12°58'N-44°51'W, 4100 m depth (Serpentine 2007).

Shrimps were collected using ROV *Victor 6000* and DSV *Nautile* slurp-guns, operated from the RVs *L'Atalante* and *Pourquoi pas?*. Prior to each

90   dive, slurp-gun bowls (shrimps sampling) and bioboxes (surrounding active chimney walls sampling) were aseptically washed with ethanol (96%) then filled with sterile seawater. Surrounding fluids were collected using 5 litres sterile bioprocess container (ThermoFischer scientific, Waltham, WI, USA) connected to peristaltic ROV pumps. Once on the vessel board, the 5 litres have been filtered under sterile conditions prior to DNA extraction.

Once on the vessel board, live shrimps were immediately dissected into body parts under sterile conditions. Guts (all sites) were carefully

95   removed from the shrimp after carapace incision from the cephalothorax to the tail. Gut samples and environmental samples (Rainbow and TAG only) were treated on board for molecular analyses (frozen), microscopic observations (glutaraldehyde processing) and *in situ* hybridization analyses (formalin processing) as detailed in Durand *et al.*, 2010 (Tab.S1).

Electron microscopic observations

Dissected gut (Tab.S1) for SEM (Scanning Electron Microscopy) and TEM (Transmission Electron Microscopy) were stained as described in Durand *et al.*, 2010. For SEM they were dehydrated by ethanol series, displayed on a specimen stub and desiccated using a critical-point dryer CPD 020 (Balzers union, Balzers, Liechtenstein). Digestive tracts were then divided longitudinally and gold-coated using a SCD 040 (Balzers union). Observations were performed with a Quanta 200 MK microscope (FEI, Hillsboro, OR, USA) and the Scandium acquisition program (Soft Imaging System, Munster, Germany). For TEM observations, samples were prepared as described in Durand *et al.*, 2010. Observations were carried out using a Zeiss 201 electron microscope operating at 80 kV.

Fluorescence in situ hybridizations

Dissected guts (Tab.S1) were prepared as described in Durand *et al.*, 2010. Sections were hybridized during 3 hours at 46°C in a 30% formamide buffer. Specimens were hybridized with the eubacterial Eub338 (Amann *et al.*, 1990) universal probe (Eurogentec, Liège, Belgium). Observations were performed with an Olympus BX61 microscope (Olympus Optical Co., Tokyo, Japan) equipped with a U-RFL-T UV light (Olympus Optical Co.) and using a Retiga 2000R camera (Qimaging, Surrey, BC, Canada) and with a Zeiss Imager.Z2 microscope (Zeiss, Oberkochen, Germany) equipped with the slider module ApoTome® (Zeiss) and the Colibri light technology (Zeiss) and using an AxioCam MRm (Zeiss) camera. Micrographs were analysed using Qcapture Pro (Qimaging) or AxioVision (Zeiss) softwares.

DNA extraction and PCR

DNA was extracted using the FastDNA® SPIN kit for soil (QBIOgen, Santa Ana, CA, USA) following the manufacturer's instructions and kept at 4°C before use for all samples (Tab.S1). Amplifications of the bacterial 16S rRNA gene were performed using universal primers E8F/U1492R (1484 bp) or E338F/U1407R (1069 bp) as detailed in Durand *et al.*, 2010.

RNA extraction and PCR

RNA was extracted using the FastRNA® SPIN kit for soil (QBIOgen) following the manufacturer's instructions and kept at -20°C before use for all samples (Tab.S1). RNA retro-transcription and amplification of the bacterial 16S rRNA gene (RT-PCR) were done using the One step® kit (Qiagen, Hilden, Germany) and the universal primers E8F/U1492R or E338F/U1407R. RT-PCR were performed with 20 ng RNA template in a 50 µl final volume using the following conditions: the RNA was retro-transcripted during 1 cycle of 30 min at 50°C, then the polymerase (HotStartTaq polymerase, Qiagen) was activated during 15 min at 95°C and finally the cDNA was amplified as detailed in Durand *et al.*, 2010 (40 cycles).

Cloning and amplified ribosomal DNA restriction analysis

PCR products were cloned using the pGEM-T (Promega, Madison, USA) or TOPO®XL (Invitrogen, Carlsbad, CA, USA) cloning kits following the manufacturer's instructions. Positive clones were PCR-amplified for control and sequenced.

Sequencing was performed at "Plateforme Biogenouest" (Roscoff, France, www.sb-roscoff.fr/SG/) using ABI prism™ 3100 GA with the Big-Dye V3.1™ Terminator technology (Applied Biosystems, Forster City, CA, USA) and by "GATC Biotech AG" (Konstanz, Germany, www.gatc-biotech.com/fr/) using ABI 3730xl with the Dye Deoxy™ Terminator technology (Applied Biosystems).

Phylogenetic analyses

130   16S rRNA phylogenetic analyses of the epibiont communities were performed on both gut and gill chamber data sets (data sets detailed in Tab.1 and Tab.2). Gut data analysed were produced from 30 *R. exoculata* as follows: 26 gut DNA and 4 gut RNA clone libraries (Tab.S1), including data sets from our previous studies (Tab. 2). The gill chamber data set was entirely compiled from previous studies (Zbinden *et al.*, 2008; Petersen *et al.*, 2010; Hügler *et al.*, 2011; Guri *et al.*, 2012), selecting only the two main gill chamber epibiont phylotypes previously described (*Epsilon*- and *Gammaproteobacteria*). Finally, five environmental DNA clone libraries were preliminary analysed for diversity and

135   included as environmental control collected at the same dives (Tab.S1).

Sequences were identified using the NCBI-BLAST program (Altschul *et al.*, 1990). They were processed and edited in Geneious Pro version 4.6 (Drummond *et al.*, 2009) and aligned using the CLUSTALW (Thompson *et al.*, 1994) algorithm. Sequences displaying more than 98% identities were clustered together and considered as single phylotype (OTU). Only homologous positions were included in final alignments. Phylogenetic constructions were performed using the parameters describing the most likely model of evolution determined by ModelTest version 3.7 (Posada

140   & Crandall, 1998) with the Akaike Information Criterion (AIC). Neighbor-joining analyses (Saitou & Nei, 1987) were conducted using PHYLO-

WIN (Galtier *et al.*, 1996). Maximum likelihood analyses (Felsenstein, 1981) were conducted using PhyML (Guindon & Gascuel, 2003) on the freely available Bioportal (www.bioportal.uio.no/). Each dataset analysis was supported by 1000 bootstrap replicates (Felsenstein, 1985).

Possible evolutionary paths among ribotypes based on the 16S rRNA gene sequence were illustrated by networks constructed using NETWORK version 4.5.1.6 (Fluxus Technology Ltd. at www.fluxus-engineering.com) with the median-joining method (Bandelt *et al.*, 1995).

145   Network stability was illustrated by two data sets for *Deferribacteres* and *Mollicutes* lineages (Fig.4b-5b A and B).

Gut sequences were named as follows: host site origin (R = Rainbow, T = TAG, L = Logatchev, A = Ashadze), number assigned to the clone sequence and the last R was for *reference* specimen as in Durand *et al.,* 2010. The digestive tract RNA clone sequence names were preceded by td. Environmental sequences were named as follows: site of origin (R = Rainbow, T = TAG), sample (S = substrate, S1 = orange chimney, S2 = black chimney, sw = seawater) and number assigned to the clone sequence. They are available from the EMBL nucleotide sequence

150   database under accession numbers FR839030 to FR839338.

Results

Macroscopic observations

155   All the collected shrimps were at the adult stage, and averaged 6 cm long at Rainbow and TAG and 4 cm at Logatchev and Ashadze sites where all individuals were smaller. They were all in anecdysis stage but were visually different, as the mineral deposit on shrimp carapaces was red on Rainbow specimens (iron-oxides), grey on TAG and Logatchev and dark black on Ashadze specimens (sulphur deposits).

Seawater temperature surrounding shrimp aggregates was between 20 and 25°C and was slightly orange-coloured and enriched in iron-oxides

160   at Rainbow and colourless to grey at TAG. The Rainbow chimney fragment RS1, close to the shrimp aggregates, was hard and covered by orange iron-oxides while both Rainbow RS2 and TAG chimneys, sampled just below the aggregates and scrapped by the shrimps, were black and crumbly (Fig.S1).

Gut microscopic observations

   Long single-celled filamentous epibionts were observed in dense population covering the gut epithelium (Fig.1b A2-B2-C2) of all

165   specimens observed here and before (Durand *et al*., 2010), whatever the site considered (Fig.1b). They were always settled between the brush cells microvilli (Fig.1b A1-B1-C1, Fig.S2), separated from gut content by the peritrophic membrane on all TEM observations. Their spiral-like shape (up to 20 µm long / less than 0.3 µm diameter) was similar regardless of the site. Ashadze epibionts morphology was slightly thinner (less than 0.2 µm diameter) and shorter on SEM observations (Fig.1b C2). Using the FISH technique, the eubacterial probe strongly hybridized on the filamentous epibionts whatever the site of origin (Fig.1b A3-B3-C3), except for the Ashadze specimen where hybridization was scarcer.

Rainbow and TAG environmental sequences

170   A preliminary molecular survey performed on Rainbow and TAG seawater and chimney samples (Tab.S1) revealed a wide diversity at the phylum and species levels (Tab.1, Tab.S2), even with this low number of clone sequences treated. Globally, the diversity of Rainbow samples was in good agreement with the one previously obtained using high throughput approach (Flores *et al.*, 2011). *Epsilonproteobacteria* and *Gammaproteobacteria* phyla were retrieved and widely distributed (Fig.2, Fig.3). Most of these clones were related to free-living forms

175 identified in marine chemosynthetic environments such as hydrothermal vents, cold seeps, mud volcanoes, whale falls or sulfidic cave, and to thiotrophic and methanotrophic hydrothermal or seep invertebrate symbionts (shrimps, mussels, gastropods, worms) (Tab.S2). EpsiB (mainly Rainbow seawater clones) and GammaA (mainly TAG seawater clones) clusters were affiliated to *R. exoculata* gill chamber epibionts from distinct sites (Petersen *et al.*, 2010; Hügler *et al.*, 2011; Guri *et al.*, 2012). Most of the other phyla retrieved here are commonly identified in hydrothermal ecosystems and are considered as ubiquitous microorganisms (Voordeckers *et al.*, 2008; Perner et al, 2007; Flores *et al.*, 2011).

180 In this study neither *Deferribacteres*-related nor *Mollicutes*-related sequences were retrieved, as to previous results from high throughput approaches (Flores *et al.*, 2011).

Global bacterial gut diversity

      The present molecular survey was performed on 30 specimens collected at the four sites (Tab.S1). This data set includes Rainbow and

185 TAG gut epibiont clone sequences obtained in two previous studies (Zbinden & Cambon-Bonavita, 2003; Durand *et al.*, 2010). A total of 2371

clones was analysed and among the 1953 (DNA) and 418 (RNA) sequences treated, low levels of gut bacterial diversity was retrieved at the phylum and species levels, compared to the environmental ones (Tab.1, Tab.S2).

Briefly, *Deferribacteres*, *Mollicutes* and *Epsilonproteobacteria* were retrieved in all libraries regardless of the site (Tab.1) with correct coverage, as described in Durand *et al.,* 2010. Lineages were still related to the resident gut *R. exoculata* symbionts (Fig.2, Fig.3, Tab.S2) not observed

190   thus far in environmental samples (Flores *et al.,*2011), confirming previous studies (Zbinden & Cambon-Bonavita 2003, Durand *et al.*, 2010). These main groups are described in the sections below through detailed ribotype analyses. A ribotype represents several 16S rRNA sequences being identical all along the section analysed.

Firmicutes were much less represented, exept at TAG site. Clone sequences, affiliated to *Clostridiaceae* retrieved in the butterfly *Spodoptera littoralis* gut (89-90% identities) or in a methanogenic reactor (90-92% identities), were identified. Phyla usually encountered in hydrothermal

195   ecosystems (Voordeckers *et al.*, 2008; Perner *et al.*, 2007; Flores *et al.*, 2011), *Gamma-*, *Delta-*, *Beta-*, *Alpha-*, *Zetaproteobacteria*, *CFB*, *Verrucomicrobiae* and *Actinobacteria*, were poorly represented. Yet, *Gammaproteobacteria* affiliated to *R. exoculata* ectosymbionts (GammaA cluster, 99% identities, Fig.3) and *Deltaproteobacteria* (Logatchev environmental clones, 99% identities) were identified.

Ashadze libraries showed a distinct composition, the DNA library diversity being restricted to *Deferribacteres* and *Epsilonproteobacteria* while the RNA one housed nine distinct phyla (Tab.1).

200

Mollicutes-related gut epibiont diversity

The *Mollicutes* phylum was not retrieved in Ashadze DNA, TAG RNA and Logatchev RNA libraries (Tab.1). Sequences obtained from other libraries clustered in four OTUs (Fig.4a).

MolliA cluster (98-99% identities with Rainbow *R. exoculata* resident gut clones, (Zbinden & Cambon-Bonavita, 2003; Durand *et al.*, 2010) housed exclusively Rainbow epibiont sequences. MolliA cluster closest relative, shrimp gut clone (*Pestarella tyrrhena* - Demiri *et al.*, 2009), shared only 89% identities. All other clusters were retrieved at each location. MolliB cluster shared 90-94% with gut/hepatopancreas crustacean and fish clones (*Ligia oceanica* - Fraune *et al.*, 2008; *Pelteobagrus fulvidraco* - Wu *et al.*, 2010). MolliC cluster were related to *R. exoculata* resident gut clones and to the unique Logatchev environmental clone (98-99% identities) (Zbinden & Cambon-Bonavita, 2003; Durand *et al.*, 2010; Hügler *et al.*, 2010). MolliC cluster closest relative shared 98-99% identities with the unique Logatchev environmental clone (Hügler *et al.*, 2010) and 87% identities with *Alloniscus perconvexus* hepatopancreas clone (Fraune *et al.*, 2008). MolliD cluster was not retrieved in DNA analyses. RNA sequences shared 86-88% identities with isopod and fish gut clones (*Gillichtys mirabilis* - Bano *et al.*, 2007; *Porcellio scaber* - Kostanjsek *et al.*, 2007) (Tab.S2).

The ribotype analysis revealed several ribotypes clusters, distinct in Rainbow specimens compared to shrimp from other sites. MolliA cluster was represented by a single ribotype, other ribotypes representing MolliBCD cluster. Network constructions (Fig.4b A-B) showed a strong dichotomy between MolliA and MolliBCD clusters. MolliA cluster (Rainbow epibionts) showed a strong divergence among these ribotypes whereas the core representing MolliBCD cluster (TAG/Logatchev/Asahdze epibionts and a unique Rainbow sequence from Zbinden & Cambon-

Bonavita, 2003) was a star-like cluster revealing a very slight divergence between these ribotypes. Unfortunately, RNA diversity (active population) did not enable us to discriminate among the four lineages to identify the long filamentous bacteria inserted between microvilli.

Deferribacteres-related gut epibiont diversity

220   *Deferribacteres* were retrieved in all libraries (Tab.1) representing an important and active resident population, with clone sequences (Fig.5a) closely related together (99% identities) and representing a single OTU, regardless of the site.

Network constructions yet revealed distinct identity, composition and diversification patterns depending on the sites of origin (Fig.5b A-B). Logatchev and Ashadze epibionts, together with most of TAG ones, exhibited a star-like cluster topology with a homogenous ribotypes distribution around two closely related and dominant ribotypes at the core of the cluster. Contrastingly, most Rainbow ribotypes and a few TAG

225   ones were much more evenly distributed (*i.e.* a higher ribotype diversity) and characterized by much larger divergences (*i.e.* a higher nucleotide diversity).

Epsilonproteobacteria-related gill chamber and gut diversity

    R. exoculata gill chamber epibionts are mainly clustered in two phylotypes, EpsiA and EpsiB (Fig.2), regardless of the site (Petersen *et al.*, 2010; Hügler *et al.*, 2011; Guri *et al.*, 2012, Jan *et al.*, 2014). Both clusters correspond to hydrothermal chemosynthetic free-living bacteria,

230   retrieved in our environmental data set, and to previously characterized invertebrates epibionts (*R. exoculata* - Zbinden *et al.*, 2008; Petersen *et al.*, 2010; Hügler *et al.*, 2011; Guri *et al.*, 2012, amphipod *Ventiella sulfuris* - Corbari *et al.*, 2012, gastropod *Crysomallon squamiferum* - Goffredi *et al.*, 2004, galatheid crab *Shinkaia crosnieri* - Tsuchida *et al.*, 2010; Watsuji *et al.*, 2010). EpsiB cluster, which dominates gill chamber epibiont

communities, was also previously proposed to be sulfide-oxidizers (Petersen *et al.*, 2010; Hügler *et al.*, 2011; Guri *et al.*, 2012; Jan *et al.*, 2014). Most epsilonproteobacterial gut clones, representing few OTUs, also clustered within the EpsiA1, EpsiA2, and EpsiB groups (Fig.2a).

235   Other gill chamber and gut clones were less represented but more diversified and divergent. They were related to chemosynthetic free-living or invertebrate-associated bacteria affiliated to groups such as *Sulfurospirillum*, *Arcobacter*, *Campylobacter* and *Sulfurimonas* (Zbinden *et al.*, 2008; Guri *et al.*, 2012), frequently involved in the sulfur cycle. They were closely related to clone sequences of the Rainbow/TAG chimney and seawater environmental samples and so probably ingested with mineral particles.

        However, the network analyses performed on the two main clusters EpsiA and EpsiB showed a clear dichotomy between these epibiont communities and a site dependent distribution. They revealed distinct structures of EpsiA and EpsiB communities. Large divergences marked the evolutionary relationships within the EpsiA cluster whereas the EpsiB cluster showed a community structured around dominant ribotypes specific to the site of origin (Fig.2). The gut clones clustered systematically in the main ribotypes of both EpsiA and EpsiB communities according to the site of origin, never as "satellite" ribotype. Altogether, and regarding the large data sets treated for network analyses, a wider diversity was observed in Rainbow specimens.

240

Gammaproteobacteria-related gill chamber and gut diversity

245

        Two OTUs, related to sulfur-oxidizing symbionts (SOX symbionts, Jan *et al.,* 2014) and methane-oxidizing symbionts (MOX symbionts), represented this phylotype (Zbinden et al., 2008; Guri *et al.*, 2012). The SOX OTU was retrieved regardless of the site; both in gill chamber and

gut data sets, with gut clones distinct but very closely related to the gill chamber ones. In contrast, the less represented MOX OTUs were retrieved only in the gill chamber and at the CH_4-rich ultramafic-hosted sites Rainbow and Logatchev (Fig.3a).

250   The dichotomy between SOX and MOX clone sequences appeared in network construction (Fig.3b). There was no clear founder ribotype in the SOX community composed of divergent ribotypes that did not significantly cluster according to the site of origin as previously reported (Petersen *et al.*, 2010). The gut clones spanned across three ribotypes regardless of the site.

Discussion

255   Results obtained in this work and previous ones (Zbinden & Cambon-Bonavita 2003, Durand *et al.,* 2010) establish that the resident epibiont community was common whatever the site specimen analyzed and the same distinctive bacterial morphology with single long filaments inserted between microvilli of the epithelial host cells was observed. They also underline a tight association between the four resident gut symbiont lineages and the host *Rimicaris exoculata*, showing a parallel in the diversification pattern of both genome compartments. Slight differences in diversity and structure observed at the ultramafic site Rainbow may possibly be attributable to the differences in generation time

260 or environmental susceptibility of some microbial lineages. The synthesis of these observations also represent one-step further in elucidating the transmission mechanisms and pathways of the resident gut symbionts in this hydrothermal species, suggesting some kind of vertical transmission in some of them.

Sample and molecular considerations

Four MAR sites have been sampled and analysed and epibiont sequences of two other sites have been added to complete this work.

265   Due to material limitations, only Rainbow and TAG environmental samples were treated in this work.

Once on vessel board, shrimps were all alive and healthy except the six Ashadze specimens, mostly lifeless. As no shrimp aggregate was identified at this location (Fabry *et al.*, 2011), one can suppose that geochemical conditions prevailing on this site were not optimal for shrimps. Then, they may have been unhealthy at this site. Moreover, they probably have suffered from decompression, Ashadze being also the deepest site (-4100 m). This may explain the somewhat distorted epibiont morphology observed in SEM and FISH (Fig.1). This may also

270   explain the possible bias in molecular analyses that may be due to partial gut degradation during ascent and before dissection, leading to partial gut recovery for the DNA extraction dedicated sample. As for other molecular studies (Bent & Forney, 2008; Quince *et al.*, 2008) the results were not quantitative as not enough clones and samples were sequenced (Flores *et al.*, 2011). All molecular approaches can be biased and the sampling strategy can lead to different results that can be then pooled together to better describe diversity. To limit the molecular bias, all the samples have been treated using the same procedures to allow us to compare qualitatively the clone libraries, including environmental ones,

275   and compiled with literature data.

One single *Deferribacteres*-related OTU and three main *Mollicutes*-related OTUs were identified in the gut clone data sets, confirming previous studies about the resident gut diversity (Zbinden & Cambon-Bonavita, 2003; Durand *et al.,* 2010). At least two OTU were identified both in *Epsilon*- and *Gammaproteobacteria* gill chamber and gut clone data sets. Ribotype analyses among each OTU were then done to overcome this apparent low diversity. Network constructions were performed to obtain a visual representation of ribotypes relationships, not constrained

280   by the sometimes arbitrary dichotomic phylogenetic trees construction. As mutation levels are usually much higher in bacteria than in eukaryotes, these analyses were also used to identify possible recent speciation events among the epibiont community.

Evolutionary relationships among epibiont communities

A striking congruence is observed here between the pattern of phylogenetic diversification observed through network reconstruction at the ribotype level of *Deferribacteres* and *Mollicutes* gut epibiont and the star-like pattern previously reported for the host shrimp and interpreted as a

285   recent and common bottleneck-expansion history across MAR sites (Teixera *et al.*, 2011, 2012). Altogether, these results suggested a recent diversification event from a small population, possibly following a bottleneck or a founder event paralleling that of the host population, except in Rainbow where stronger divergence suggested a more ancient history.

The network topologies indeed highlighted a very particular signature of deeper divergence and higher diversity at Rainbow suggesting a distinct epibiont evolutionary history. In contrast, the epibiont community networks structure from Logatchev site identified one main ribotype

290   from which "satellite" ribotypes have recently emerged. The same result was observed for the few Ashadze samples analysed. In a population, this is a typical signature produced by a recent event increasing the selective pressure on the main strain (represented by the main ribotype), or to a recent diversification through demographic expansion (Cohan, 2004). The structure of TAG epibiont populations seemed to be intermediate, harbouring one main ribotype and several "satellites". These results tend to propose an ancient evolutionary history for *R. exoculata* gut epibiosis from Rainbow, then for TAG, and finally a recent and common expansion at Logatchev and Ashadze sites. This history

295   would not be linked to the sites geochemistry but appear in line with suggested fluctuation of population size in the host demographic history (Teixeira *et al.*, 2011, 2012).

The four resident lineages diversity was rather homogeneous across these three last sites, despite the physical barriers such as distance, depth and contrasted geochemical conditions prevailing in the MAR sites. The host phylogeography (Petersen *et al.*, 2010; Texeira *et al.*, 2011, 2012) revealed no site-segregation suggesting significant recurrent or recent gene flow among *R. exoculata* populations over vast geographic

300   distances and a very recent divergence history. Yet in Rainbow, the epibiont divergence pattern at the ribotype level contrasts with that of the hosts. Both demographic and selective processes may explain this particular position of Rainbow. Demographic events that would have already impacted the microbial genome but would be too recent to have imprinted the host one, owing to differences in life span, population sizes resulting in evolutionary kinetic differences, as suggested in Teixeira *et al.* (2011). Now, difference in the level of physical isolation and/or specificity of environmental conditions would also be possible owing to the Rainbow site location on the MAR Azorean segment and on the

305   internal side of a nodal basin (Fig.S3). This area could be partially protected from deep-oceanic currents and the Azorean plateau proximity could generate convection movements in deep-oceanic water flows (Wolanski & Hamner, 1988), creating a physically and biologically relatively isolated area. Besides, the unique geochemical conditions prevailing in Rainbow could be a factor affecting the selective pressures acting on epibionts. Rainbow is also the shallowest site (less than 3000 m depth). The abyssal regions are considered beyond 3000 m depth, and associated changes in physical parameters might also constitute a biological (Priede *et al.*, 2006) and/or environmental barrier for some

310   species.

Possible transmission pathways of gut epibiont communities

Phylogenetic analyses of the *Gammaproteobacteria* group did not reveal spatial segregation, as sequences always clustered in the larger hydrothermal symbiont group, and were closely related to clones retrieved in the seawater surrounding shrimp aggregates. Nevertheless, the epibiont diversity was clearly reduced regarding the environmental one, even with few clones analyzed. This suggests at least an efficient

315   filtering process of gammaproteobacterial gut clones, as well as gill chamber ones, could they be acquired from the environment after selective filtering. Similarly, the two *Epsilonproteobacteria* epibiont lineages, EpsiA and EpsiB, all clustering in the hydrothermal symbionts group, exhibited few OTUs, also suggesting a selective filtering process from an environmental pool, as observed for the gill chamber (Petersen *et al.*, 2010). EpsiB population was structured around site-dependant ribotypes. Together with the panmixia observed at the host level phylogeography (Teixera *et al.*, 2011, 2012), this suggests that site-dependent processes may act on those symbionts. Besides,

320   *Epsilonproteobacteria* gut and gill chamber epibionts were similar, further suggesting gut ones could be directly acquired from the environment or ingested from the gill chamber. It may thus be a transient community remaining thanks to a permanent renewal from the gill chamber. All these results related to *Proteobacteria* symbionts can also be compared to what is observed in *Bathymodiolus* (DeChaine *et al.*, 2006; Van der Heijden *et al.*, 2012) where a continuous environmental symbiont acquisition would be the rule, probably implying a control or selection by the host. If for *Bathymodiolus* species no genes have been identified yet for symbiont communication or host control (Van der Heijden *et al.*, 2012),

325   an antimicrobial peptide has been identified for *Alvinella pompejana* symbiont control (Tasiemski *et al.,* 2014). This could be the role of *Lux* genes and a crustine-like gene retrieved respectively for epibionts and *R. exoculata* (Jan *et al.*, 2014; Cottin *et al.*, 2010) avoiding then symbiont proliferation.

Contrastingly, *Mollicutes* and *Deferribacteres* relatives showed network topology in line with that of the host, and have not yet been retrieved in the free-living microbial community (Flores *et al.*, 2011) except for one clone collected close to shrimp aggregate (Hügler *et al.*,

330 2010). All those OTUs represent potentially new species. Only one *Deferribacteres* and three *Mollicutes* OTUs were retrieved in gut libraries whatever the site considered (MolliB to MolliD clusters), MolliA cluster being Rainbow-specific. This suggests that those bacterial lineages could be acquired either horizontally or vertically. A horizontal transmission would imply an efficient growth in the gut where they are easily detected, but not in the environment, where they are almost not retrieved even using high throuput approaches (Flores *et al.*, 2011). Moreover free-living bacteria are usually more divergent over distant sites. The low divergence observed here would be attributable to a mechanism impeding

335 divergence, such as a strong specific host-symbiont recognition/control system. Vertical transmission would suggest the low site influence at the species level as a result of the apparent large scale dispersal or very recent common history of their hosts (Teixera *et al.*, 2011, 2012), the compared network phylogenies supporting a tightly entangled evolution of those lineages as that of their hosts as described above. As reviewed in Bright & Bulgheresi, 2010, several ways of vertical transmission could be suggested, from the tight co-evolution resulting from egg transmission to an evolutionary looser transmission during spawning or trophallaxis. Epibionts could be (1) acquired at early juvenile stages by

340 processes such as oral or anal trophallaxis as adults are closely surrounding recruited juveniles where long filamentous bacteria have also been observed in the gut (Fig.S2). (2) externally-transmitted with eggs, embedded in a mucous structure containing the microorganisms, but not identified yet (Guri *et al.*, 2012). (3) Transmitted from maternal germ cells inside the eggs. The first two scenarios imply that part of the transmitted epibionts pool would be released in the surrounding environment and occasionally retrieved depending on the dilution process. This could also explain the unique *Mollicutes*-related environmental clone retrieved in seawater collected above a mussel bed surrounding *R.*

345　*exoculata* populations at Logatchev (Fig.S1e; Hügler *et al.*, 2010). So, this seawater sample could have contained *Mollicutes*-related bacteria coming from faeces or eggs/larvae. In the last scenario of a strict vertical transmission through the eggs, larvae would be colonised before they hatch, leading to a common dispersion pathway of the host and its symbionts as the one suggested by their compared network phylogenies. Larval stages are supposed to be pelagic, capable of long distance dispersal (Pond *et al.*, 1997, 2000). These results would argue in favour of important gene flows among geographically distinct populations affecting both host and symbionts. Present results favour a kind of vertical

350　transmission, yet disentangling the three possible scenarios requires future collect efforts followed by analyses of eggs and early developmental stages.

The holobiont fitness

　　　The holobiont is the sum of capabilities of the host and its symbionts (Zilber-Rosenberg & Rosenberg, 2008). From a metabolic point of view, *R. exoculata*, which ingests mostly minerals, relies on its symbionts for nutrition (Ponsard *et al.*, 2013), as insects subsisting on

355　nutritionally-poor or low energy habitats which are supplied in essential compounds produced by symbiont metabolisms (Dillon & Dillon, 2004 for review). Such association is suggested to improve holobiont fitness and invasive power of introduced species (Nardon, 1999; Zilber-Rosenberg & Rosenberg, 2008). Even if no metabolism could be inferred on the basis of 16S rRNA gene, first hypotheses can be proposed according to the phyla identified.

　　Epsilonproteobacteria and *Gammaproteobacteria* are known in environmental libraries (Campbell *et al.*, 2006; Flores *et al.*, 2011). All gut

360　relatives were related to free-living environmental clones or to invertebrate symbionts from sulphides, methane, iron and hydrogen enriched

ecosystems (Tab.S2), fitting well the geochemical conditions prevailing in the four sites studied. These results together with previous studies (Zbinden *et al.*, 2008; Petersen *et al.*, 2010; Hügler *et al.*, 2011; Guri *et al.*, 2012; Ponsard *et al.*, 2013; Jan *et al.*, 2014) confirmed they are probably involved in sulphur (Ponsard *et al.*, 2013), and could be involved in methane, iron and/or hydrogen cycles. In particular the *Gammaproteobacteria* distribution, where MOX are retrieved only at ultramafic-hosted site, may suggest adaptive process regarding

365   geochemical conditions. Such activities probably represent detoxification processes and/or nutritive intake of microbial metabolic by products for the host.

Molecular analyses confirmed that *Deferribacteres* and *Mollicutes* were tightly associated with *R. exoculata* gut. Their continuous distribution all along the MAR hydrothermal sites and their absence in most environmental libraries (this study and other) strengthened the hypothesis of resident, specific and filtered or selected bacterial community. According to molecular analyses, *Deferribacteres*-epibionts were an important

370   and active population, and could be implied in iron cycle with a possible detoxification role for the host. Cuticle fragments are sometimes observed in the digestive content and could be difficult to digest. *Deferribacteres*, some being known to be heterotrophic micro-organisms (Greene *et al.*, 1997; Miroshnichenko *et al.*, 2003; Takai *et al.*, 2003), could then play a complementary role in cuticle hydrolysis, bringing nutrients to the host and the epibiont community. *Mollicutes* were present at the four sites in different gut ecosystems, but yet their metabolic role is still not elucidated (Kostanjsek *et al.*, 2007; Fraune & Zimmer, 2008).

375   The holobiont is also a sum of genomes which must communicate. The filamentous bacteria inserted between microvilli of healthy epithelial gut cells of all specimens observed so far were all single-celled (Fig.1) and seemed to be shorter in small juveniles (Fig.S2). The resident community is still restricted to four lineages. All those observations could be the result of an effective host invasion control. This has been

described for insects (Anselme *et al.*, 2008) and recently for another deep sea hydrothermal vent symbiotic invertebrate, *Alvinella pompejana* (Tasiemski *et al.,* 2014) harbouring dorsal epibionts. The presence of those dorsal epibionts was shown to enhance the antimicrobial peptide

380   synthesis. This would then avoid bacterial cell proliferation thanks to an efficient epibiont control and selection by the host. Penaeideae shrimps are known to synthesise antimicrobial peptides (Bachère *et al.*, 2004; Cuthbertson *et al.*, 2008). This could also be the case for the Alvinocaridideae *R. exoculata* shrimp enabling the shrimp to limit symbionts colonisation in strict locations such as the gill chamber and between the epithelial microvilli.

385   In order to complete this study, other sites should be explored to construct the holobiont evolutionary and expansion history that seems to be more ancient at Rainbow, the northern part of the known shrimp expansion in our study. In order to improve the understanding of the shrimp life cycle, an effort to collect larvae and early juvenile stages should be done. High throughput sequencing approaches will also allow a better screening for possible free-living forms of the gut-resident epibionts (*Deferribacteres* and *Mollicutes*). This study suggests the gut microbial colonization universality and the key role they could play in healthy hosts.

390

Supplementary information is available at *The FEMS Microbiol Ecol Journal* website.

Acknowledgements

References

Altschul SF, Gish W, Miller W, Myers EW & Lipman DJ (1990) Basic local alignment search tool. *J. Mol. Biol.* **215**:403-410.

Amann RI, Binder BJ, Olson RJ, Chisholm SW, Devereux R & Stahl DA (1990) Combination of 16S rRNA-targeted oligonucleotide probes with flow cytometry for analyzing mixed microbial populations. *Appl. Environ. Microbiol.* **56**:1919-1925.

405 Anselme C, Pérez-Brocal V, Vallier A, Vincent-Monegat C, Charif D, Latorre A, *et al.* (2008) Identification of the Weevil immune genes and their expression in the bacteriome tissue. *BMC Biol.* **6**:43.

Bachère E, Gueguen Y, Gonzalez M, de Lorgeril J, Garnier J & Romestand B (2004) Insights into the anti-microbial defense of marine invertebrates: the penaeid shrimps and the oyster *Crassostrea gigas*. *Immunol. Rev.* **198**:149-168.

Bandelt HJ, Forster P, Sykes BC & Richards MB (1995) Mitochondrial portraits of human populations using median networks. *Genetics*
410 **141**:743-753.

Bano N, deRae Smith A, Bennett W, Vasquez L & Hollibaugh JT (2007) Dominance of Mycoplasma in the guts of the long-jawed mudsucker, *Gillichtys mirabilis*, from five California salt marshes. *Env. Microbiol.* **9**(10):2636-2641.

Bent SJ & Forney LJ (2008) The tragedy of the uncommon: understanding limitations in the analysis of microbial diversity. *The ISME J.* **2**:689-695.

415 Brazelton WJ, Ludwig KA, Sogin ML, Andreishcheva EN, Kelley DS Shen CC, *et al.* (2010) Archaea and Bacteria with surprising microdiversity show shifts in dominance over 1,000-year time scales in hydrothermal chimneys. *Proc. Natl. Acad. Sci.* **107**(4):1612-1617.

Bright M, Bulgheresi S. (2010) A complex journey: transmission of microbial symbionts. Nat Rev Microbiol. Mar;8(3):218-30. doi: 10.1038/nrmicro2262.

Campbell BJ, Summers Engel A, Porter ML & Takaï K (2006) The versatile ε-proteobacteria: key players in sulphidic habitats. *Nature* **4**:458-
420 468.

Casanova B, Brunet M & Segonzac, M. (1993) L'impact d'une épibiose bactérienne sur la morphologie fonctionnelle des crevettes associées à l'hydrothermalisme médio-Atlantique. *Cah. Biol. Mar.* **34**:573-588.

Charlou JL, Donval JP, Fouquet Y, Jean-Baptiste P & Holm N (2002) Geochemistry of high H_2 and CH_4 vent fluids issuing from ultramafic rocks at the Rainbow hydrothermal field (36°14'N, MAR). *Chem. Geol.* **191**:345-359.

425   Charlou JL, Donval JP, Konn C, Ondreas H, Jean-Baptiste P, Fourre E & Fouquet Y (2010) High Production and fluxes of H_2 and CH_4 and evidence of abiotic hydrocarbon synthesis by serpentinization in ultramafic-hosted hydrothermal systems on the Mid-Atlantic Ridge. *AGU Monograph Ser.* pp.265-296.

Cohan FM (2004) Concepts of bacterial biodiversity for the age of genomics. In: C.M. Fraser, T. Read, and K.E. Nelson (ed). Microbial Genomes. Humana Press: Totowa, pp 175-194.

430   Corbari L, Cambon-Bonavita MA, Long GJ, Zbinden M, Gaill F & Compère P (2008a) Iron oxide deposits associated with the ectosymbiotic bacteria in the hydrothermal vent shrimp *Rimicaris exoculata*. *Biogeosciences* **5**: 1295-1310.

Corbari L, Zbinden M, Cambon-Bonavita MA, Gaill F & Compère P (2008b) Bacterial symbionts and mineral deposits in the branchial chamber of the hydrothermal vent shrimp *Rimicaris exoculata*: relationship to moult cycle. *Aquat. Biol.* **1**:225-238.

Corbari L, Durand L, Cambon-Bonavita MA, Gaill F & Compère P (2012) New digestive symbiosis in the hydrothermal vent amphipoda *Ventiella*
435   *sulfuris*. *C. R. Biol.* **355**:142-154.

Cottin D, Shillito B, Chertemps T, Thatje S, Léger N & Ravaux J (2010) Comparison of heat-shock responses between the hydrothermal vent shrimp *Rimicaris exoculata* and the related coastal shrimp *Palaemonetes varians*. Journal of Experimental Marine Biology and Ecology: 393, 9-16

Cuthbertson BJ, Deterding LJ, Williams JG, Tomer KB, Etienne K, Blackshear PJ, *et al.* (2008) Diversity in penaeidin antimicrobial peptide form
440   and function. *Dev. Comp. Immunol.* **32**(3):167-181.

DeChaine EG, Bates AE, Shank TM and Cavanaugh MC (2006) Off-axis symbiosis found: characterization and biogeography of bacterial symbionts of B*athymodiolus* mussels from Lost City hydrothermal vents. Environmental Microbiology 8(11), 1902–1912.

Demiri A, Meziti A, Papaspyrou S, Thessalou-Legaki M & Kormas KA (2009) Abdominal setae and midgut bacteria of the mudshrimp *Pestarella tyrrhena*. *Cent. Eur. J. biol.* **4**(4):558-566.

445   Desbruyères D, Biscoito M, Caprais JC, Colaço A, Comtet T, Crassous P, *et al*. (2001) Variations in deep-sea hydrothermal vent communities on the Mid-Atlantic Ridge near the Azores plateau. *Deep-sea Res. Pt I* **48**:1325-1346.

Dillon RJ & Dillon VM (2004) The gut bacteria of insects: nonpathogenic interactions. *Annu. Rev. Entomol.* **49**:71-92.

Drummond AJ, Ashton B, Cheung M, Heled J, Kearse M, Moir R, *et al.* (2009) Geneious v4.8, Available from http://www.geneious.com/

Durand L, Zbinden M, Cueff-Gauchard V, Duperron S, Roussel EG, Shillito B, *et al*. (2010) Microbial diversity associated with the hydrothermal
450   shrimp *Rimicaris exoculata* gut and occurrence of a resident microbial community. *FEMS Microbiol. Ecol.* **71**:291-303.

Fabri MC, Bargain A, Briand P, Gebruk A, Fouquet Y, Morineaux M, *et al*. (2011) The hydrothermal vent community of a new deep-sea field, Ashadze-1, 12°58'N on the Mid-Atlantic Ridge. *J. Mar. Biol. Assoc. UK* **91**(1):1-13.

Felsenstein J (1981) Evolutionary trees from DNA sequences: a maximum likelihood approach. *J. Mol. Evol.* **17**:368-376.

Felsenstein J (1985) Confidence limits on phylogenies: an approach using the bootstrap. *Evol.* **30**:783-791.

455   Flores GE, Campbell JH, Kirshtein JD, Meneghin J, Podar M, Steinberg JI, *et al*. (2011) Microbial community structure of hydrothermal deposits from geochemically different vent fields along the Mid-Atlantic Ridge. *Env. Microbiol.* **13**:no. doi:10.1111/j.1462-2920.2011.02463.x.

Fouquet Y, Cherkashov G, Charlou JL, Ondréas H, Birot D, Cannat M, *et al*. (2008) Serpentine cruise – ultramafic hosted hydrothermal deposits on the Mid-Atlantic Ridge : First submersible studies on Ashadze 1 and 2, Logatchev 2 and Krasnov vent fields. *InterRidge News* **17**:15-19.

Fraune S & Zimmer M (2008) Host specificity of environmentally transmitted *Mycoplasma*-like isopod symbionts. *Env. Microbiol.* **10**(10):2497-
460   2504.

Galtier N, Gouy M & Gautier C (1996) SEAVIEW and PHYLO_WIN: two graphic tools for sequence alignment and molecular phylogeny: *CABIOS* **12**:543-548.

Gebruk AV, Southward EC, Kennedy H & Southward AJ (2000) Food sources, behaviour, and distribution of hydrothermal vent shrimps at the Mid-Atlantic Ridge. *J. Mar. Biol. Assoc. UK* **80**:485-499.

465 Goffredi SK, Warén A, Orphan V, Van Dover CL & Vrijenhoek C (2004) Novel forms of structural integration between microbes and a hydrothermal vent gastropod from the Indian Ocean. *Appl. Env. Microbiol.* **70**(5):3082-3090.

Green AC, Patel BKC & Sheeny AJ (1997) *Deferribacter thermophilus* gen. nov., sp. nov., an novel thermophilic manganese- and iron-reducing bacterium isolated from a petroleum reservoir. *Int. J. Syst. Evol. Microbiol.* **47**(2): 505-509.

Guindon S & Gascuel O (2003) A simple, fast, and accurate algorithm to estimate large phylogenies by maximum likelihood. *Syst. Biol.*
470 **52**(5):696-704.

Guri M, Durand L, Cueff-Gauchard V, Zbinden M, Crassous P, Shillito B & Cambon-Bonavita MA (2012) Acquisition of epibiotic bacteria along the life cycle of the hydrothermal shrimp *Rimicaris exoculata*. *The ISME J.* **6**:597-609.

Hasegawa M, Kishino K & Yano T (1985) Dating the human-ape splitting by a molecular clock of mitochondrial DNA. *J. Mol. Evol.* **22**:160-174.

Heddi A, Charles H, Khatchadourian C, Bonnot G & Nardon P (1998) Molecular characterization of the principal symbiotic bacteria of the weevil
475 *Sitophilus oryzae*: a peculiar G+C content of an endocytobiotic DNA. *J. Mol. Evol.* **47**:52-61.

Hügler M, Gärtner A & Imhoff JF (2010) Functional genes as markers for sulfur cycling and CO_2 fixation in microbial communities of hydrothermal vents of the Logatchev field. *FEMS Microbiol. Ecol.* **73**:526-537.

Hügler M, Petersen G, Dubilier N, Imhoff J & Sievert SM (2011) Pathways of carbon and energy metabolism of the epibiotic community associated with the deep-sea hydrothermal vent shrimp *Rimicaris exoculata*. *PLoS One* **6**(1):e16018. doi:10.1371/journal.pone.0016018.

480   Jan C, Petersen J, Werner J, Huang S, Teeling H, Glöckner FO, Golyshina OV, Dubilier N, Golyshin PN, Jebbar M & Cambon-Bonavita MA (2014) The gill chamber epibiosis of deep-sea *Rimicaris exoculata* shrimp revisited by metagenomics and discovery of zetaproteobacterial epibionts. *Environ microbiol*, **16**: 2723-2738.

Jukes TH & Cantor CR (1969) Evolution of protein molecules. In: Munro H.N. (ed) *Mammalian protein metabolism, III*. New York: Academic Press, pp 21-132.

485   Kelley DS, Karson JA, Blackman DK, Früh-Green GL, Butterfield DA, Lilley MD, *et al.* (2001) An off-axis hydrothermal vent field near the Mid-Atlantic Ridge at 30 degrees N. *Nature* **412**:145-149.

Kimura M (1980) A simple method for estimating evolutionary rate of base substitution through comparative studies of nucleotide sequences. *J. Mol. Evol.* **16**:111-120.

Komaï T & Segonzac M (2008) Taxonomic review of the hydrothermal vent shrimp genera *Rimicaris* Williams & Rona and *Chorocaris* Martin &
490   Hessler (Crustacea: Decapoda: Caridea: Alvinocarididea). *J. Shellfish Res.* **27**(1):21-41.

Kostanjsek R, Strus J & Augustin G (2007) "*Candidatus* Bacilloplasma", a novel lineage of *Mollicutes* associated with the hindgut wall of the terrestrial isopod *Porcellio scaber* (Crustacea: Isopoda). *Appl. Env. Microbiol.* **73**(17):5566-5573.

López-García P, Philippe H, Gaill F & Moreira D (2003) Autochthonous eukaryotic diversity in hydrothermal sediment and experimental microcolonizers at the Mid-Atlantic Ridge. *Proc. Natl. Acad. Sci.* USA **100**:697-702.

495   Miroshnichenko ML, Slobodkin AI, Kostrikina NA, L'Haridon S, Nercessian O, Spring S, *et al.* (2003) *Deferribacter abyssi* sp. nov., an anaerobic thermophile from deep-sea hydrothermal vents of the Mid-Atlantic Ridge. *Int. J. Syst. Evol. Microbiol.* **5**: 1637-1641.

Nardon P (1999) Symbiosis as an example of an acquired character: neolamarckism of neodarwinism? *Bull. Soc. Zool. France* 124:39-52.

Nye V, Copley J & Plouviez S (2012) A new species of *Rimicaris* (Crustacea: Decapoda: Caridea: Alvinocarididea) from hydrothermal vent fields on the Mid-Cayman Spreading Centre, Caribbean. *J. Mar. Biol. Assoc. UK* doi: 10.1017/S.0025315411002001.

500   Perner M, Kuever J, Seifert R, Pape T, Koschinsky A, Schmidt K, *et al.* (2007) The influence of ultramafic rocks on microbial communities at the Logatchev hydrothermal field, located 15°N on the Mid-Atlantic Ridge. *FEMS Microbiol. Ecol.* **61**:97-109.

Petersen JM, Ramette A, Lott C, Cambon-Bonavita MA, Zbinden M & Dubilier N (2010) Dual symbiosis of the vent shrimp *Rimicaris exoculata* with filamentous *Gamma*- and *Epsilonproteobacteria* at four Mid-Atlantic Ridge hydrothermal vent fields. *Environ. Microbiol.* **12**(8):2204-2218.

Polz M, & Cavanaugh C (1995) Dominance of one bacterial phylotype at a Mid-Atlantic Ridge hydrothermal vent site. *Proc. Natl. Acad. Sci.*
505   **92**:7232-7236.

Polz M, Robinson JJ, Cavanaugh C & Van Dover CL (1998) Trophic ecology of massive shrimp aggregations at a Mid-Atlantic Ridge hydrothermal vent site. *Limnol. Oceanogr.* **43**:1631-1638.

Pond D, Dixon D & Sargent J (1997) Wax-ester reserves facilitate dispersal of hydrothermal vent shrimps. *Mar. Ecol. Prog. Ser.* **146**:289–290.

Pond DW, Gebruk A, Southward EC, Southward AJ, Fallick AE, Bell MV, *et al.* (2000) Unusual fatty acid composition of storage lipids in the
510   bresilioid shrimp *Rimicaris exoculata* couples the photic zone with MAR hydrothermal vent sites. *Mar. Ecol. Prog. Ser.* **198**:171–179.

Ponsard J, Cambon-Bonavita MA, Zbinden M, Lepoint G, Joassin A, Corbari L, Shillito B, Durand L, Cueff-Gauchard V & Compere P (2013) Inorganic carbon fixation by chemosynthetic ectosymbionts and nutritional transfers to the hydrothermal vent host-shrimp *Rimicaris exoculata.* The *ISME J.* **7**:96-109.

Posada D & Crandall KA (1998) MODELTEST: testing the model of DNA substitution. *Bioinformatics* **14**(9):817-818.

515   Priede IG, Froese R, Bailey DM, Bergstad OA, Collins MA, Dyb JE, *et al.* (2006) The absence of sharks from abyssal regions of the world's oceans. *Proc. R. Soc. Lond. Ser. B.* **273**:1435-1441.

Quince C, Curtis TP & Sloan WT (2008) The rational exploration of microbial diversity. *The ISME J.* **2**:997-1006.

Ravaux J, Cottin D, Chertemps T, Hamel G & Shillito B (2009) Hydrothermal vent shrimps display low expression of the heat-inducible *hsp70* gene in nature. *Mar. Ecol. Prog. Ser.* **396**:153-156.

520   Roussel EG, Konn C, Charlou JL, Donval JP, Fouquet Y, Querellou J, *et al.* (2011) Comparison of microbial communities associated with three Atlantic ultramafic hydrothermal systems. *FEMS Microbiol. Ecol.* doi: 10.1111/j.1574-6941.2011.01161.x.

Saitou N & Nei M (1987) The neighbor-joining method: a new method for reconstructing phylogenetic trees. *Mol. Biol. Evol.* **4**:406-425.

Schmidt C, Vuillemin R, Le Gall C, Gaill F & Le Bris N (2008) Geochemical energy sources for microbial primary production in the environment of hydrothermal vent shrimps. *Mar. Chem.* **108**:18-31.

525   Segonzac M, de Saint Laurent M & Casanova B (1993) L'énigme du comportement trophique des crevettes Alvinocarididae des sites hydrothermaux de la dorsale médio-Atlantique. *Cah. Biol. Mar.* **34:**535-571.

Takaï K, Kobayashi H, Nealson KH & Horikoshi K (2003) *Deferribacter desulfuricans* sp. nov., a nover sulphur-, nitrate- and arsenate-reducing thermophile isolate from a deep-sea hydrothermal vent. *Int. J. Syst. Evol. Microbiol.* **53**(3):839-846.

Tasiemski A, Jung S, Boidin-Wichlacz C, Jollivet D, Cuvillier-Hot V, Pradillon F, Vetriani,C Hecht O, Sönnichsen FD, Gelhaus C, Hung CW,
530   Tholey A, Leippe M, Grötzinger J, Gaill F (2014) Characterization and Function of the First Antibiotic Isolated from a Vent Organism: The Extremophile Metazoan *Alvinella pompejana*. PLoS ONE 9(4): e95737. 0.1371/journal.pone.0095737

Teixeira S, Cambon-Bonavita MA, Serrão EA, Desbruyères D & Arnaud-Haond S (2011) Recent population expansion and connectivity in the hydrothermal shrimp *Rimicaris exoculata* along the Mid-Atlantic Ridge. *J. Biogeography* **38**:564-574.

Teixeira S, Serrão EA, Arnaud-Haond S (2012) Panmixia in a fragmented and unstable environment: the hydrothermal shrimp *Rimicaris
535   exoculata* disperses extensively along the Mid-Atlantic Ridge. PLoS ONE. **7**(6): e38521. doi:10.1371/journal.pone.0038521

Thompson JD, Higgins DG & Gibson TJ (1994) Clustal W: improving the sensitivity of progressive multiple sequence alignment through sequence weighting, position-specific gap penalties and weight matrix choice. *Nucleic Ac. Res.* **22**:4673-4680.

Tsuchida S, Suzuki Y, Fujiwara Y, Kawato M, Uematsu K, Yamanaka T, *et al*. (2010) Epibiotic association between filamentous bacteria and the vent-associated galatheid crab, *Shinkaia crosnieri* (Decapoda: Anomura). *J. Mar. Biol. Assoc. UK* **91**(1):23-32.

540   Van der Heijden K, Petersen JM, Dubilier N, Borowski C (2012) Genetic Connectivity between North and South Mid-Atlantic Ridge Chemosynthetic Bivalves and Their Symbionts. PLoS ONE 7(7) e39994.

Van Dover CL, Fry B, Grassle JF, Humphris S & Rona PA (1988) Feeding biology of the shrimp *Rimicaris exoculata* at hydrothermal vents on the Mid-Atlantic Ridge. *Mar. Biol.* **98**:209-216.

Voordeckers JW, Do MH, Hügler M, Ro V, Sievert SM & Vetriani C (2008) Culture dependant and independent analyses of 16S rRNA and ATP
545   citrate lyase genes: a comparison of microbial communities from different black smoker chimneys on the Mid-Atlantic Ridge. *Extremophiles* **12**:627-640.

Watabe H & Hashimoto J (2002) A new species of the genus *Rimicaris* (Alvinocarididae: Caridea: Decapoda) from the active hydrothermal vent field, 'Kairei Field', on the Central Indian Ridge, Indian Ocean. *Zool. Sci.* **19**:1167-1174.

Watsuji T, Nakagawa S, Tsuchida S, Toki T, Hirota A, Tsunogai U, *et al*. (2010) Diversity and function of epibiotic microbial communities on the
550   Galatheid Crab, *Shinkaia crosnieri*. *Microbes Environ.* **25**(4):288-294.

Williams AB & Rona PA (1986) Two new caridean shrimps (bresiliidae) from a hydrothermal field on the Mid-Atlantic Ridge. *J. Crust. Biol.* **6**:446-462.

Wolanski E & Hamner M (1988) Topgraphically controlled fronts in the ocean and their biological influence. *Science* **241**(4862):177-181.

Wu S, Gao T, Zheng Y, Wang W, Cheng Y & Wang G (2010) Microbial diversity of intestinal contents and mucus in yellow catfish (*Pelteobagrus*
555   *fulvidraco*). *Aquacult.* **303**:1-7.

Zbinden M & Cambon-Bonavita MA (2003) Occurrence of *Deferribacterales* and *Entomoplasmatales* in the deep-sea Alvinocarid shrimp *Rimicaris exoculata* gut. *FEMS Microbiol. Ecol.* **46**:23-30.

Zbinden M, Le Bris N, Gaill F & Compere P (2004) Distribution of bacteria and associated minerals in the gill chamber of the vent shrimp *Rimicaris exoculata* and related biogeochemical processes. *Mar. Ecol. Prog. Ser.* **284**:237-251.

560   Zbinden M, Shillito B, Le Bris N, De Villardi de Montlaur C, Roussel E, Guyot F, *et al.* (2008) New insights in metabolic diversity among the epibiotic microbial communities of the hydrothermal shrimp *Rimicaris exoculata*. *J. Exp. Mar. Biol. Ecol.* **359**:131-140.

Zilber-Rosenberg I & Rosenberg E (2008) Role of microorganisms in the evolution of animals and plants: the hologenome theory of evolution. *FEMS Microbiol. Rev.* **32**:723-735.

565

Table 1 - Distribution of the bacterial 16S rRNA gene and transcribed 16S rRNA clones associated with the reference shrimp guts and the environment at the four studied hydrothermal sites. This data set was provided from this study (a) and previous ones (b= this study, Durand *et al.*, 2010 and Zbinden & Cambon-Bonavita, 2003; c = this study, Durand *et al.*, 2010)

Phylogenetic groups		Number of clones									
		Reference *R. exoculata* specimens				Environmental samples (DNA)					
		Rainbow	TAG	Logatchev [a]	Ashadze [a]	Rainbow seawater [a]	Rainbow orange chimney [a]	Rainbow black chimney [a]	TAG seawater [a]	TAG chimney [a]	Total
Deferribacteres	DNA	165 [b]	220 [c]	150	127	0	0	0	0	0	662
	RNA [a]	137	72	84	4	-	-	-	-	-	297
Mollicutes	DNA	51 [b]	97 [c]	123	0	0	0	0	0	0	271
	RNA [a]	12	0	0	40	-	-	-	-	-	52
Epsilonproteobacteria	DNA	75 [b]	113 [c]	152	69	50	46	35	26	22	588
	RNA [a]	22	1	1	3	-	-	-	-	-	27
Gammaproteobacteria	DNA	78 [b]	3 [a]	9	0	5	22	18	38	36	209
	RNA [a]	0	0	0	6	-	-	-	-	-	6
Alphaproteobacteria	DNA	0	4 [a]	0	0	0	5	10	5	17	41
	RNA [a]	0	0	0	0	-	-	-	-	-	0
Deltaproteobacteria	DNA	0	2 [a]	6	0	1	1	8	3	2	23
	RNA [a]	1	0	0	10	-	-	-	-	-	11
Betaproteobacteria	DNA	1 [a]	1	0	0	0	0	6	4	0	12
	RNA [a]	0	0	0	2	-	-	-	-	-	2
Zetaproteobacteria	DNA	0	0	1	0	0	0	2	2	0	5
	RNA [a]	0	0	0	0	-	-	-	-	-	0
CFB	DNA	4 [c]	3 [c]	3	0	4	5	3	4	5	31
	RNA [a]	5	1	0	1	-	-	-	-	-	7
Verrucomicrobiae	DNA	0	6 [c]	2	0	0	0	0	0	1	9
	RNA [a]	0	0	0	0	-	-	-	-	-	0
Firmicutes	DNA	9 [b]	69 [c]	0	0	0	0	1	0	0	79
	RNA [a]	0	12	0	0	-	-	-	-	-	12

Actinobacteriae	DNA	0	0	2	0	0	0	0	0	0	2
	RNA[a]	0	0	0	2	-	-	-	-	-	2
Thermodesulfobacteres	DNA	0	0	0	0	0	3	1	0	0	4
	RNA[a]	0	0	0	0	-	-	-	-	-	0
Aquificales	DNA	0	0	0	0	0	1	2	0	0	3
	RNA[a]	0	0	0	0	-	-	-	-	-	0
Chloroflexi	DNA	0	1[a]	0	0	0	0	0	0	0	1
	RNA[a]	0	0	0	0	-	-	-	-	-	0
Unaffiliated	DNA	0	1[a]	6	0	0	3	0	3	0	13
	RNA[a]	0	0	0	2	-	-	-	-	-	2
Total	DNA	383	520	454	196	60	86	86	85	83	1953
	RNA	177	86	85	70	-	-	-	-	-	418

Table 2 - Distribution of the 16S rRNA gene sequences of *Epsilon*- and *Gammaproteobacteria*-related epibionts associated with the gill chamber and the gut, used for phylogenetic analyses (trees and networks). These 16S rRNA gene sequences were obtained from shrimps sampled at six hydrothermal sites.

570

| Site | Number of gill chamber clones | | Reference |
	Epsilonproteobacteria	*Gammaproteobacteria*	
Rainbow	38	15	Zbinden *et al.*, 2008
	6	6	Petersen *et al.*, 2010
	31	8	Guri *et al.*, 2012
	51	11	*This study*
TAG	6	3	Petersen *et al.*, 2010
	57	2	*This study*
Snake Pit	1	0	Polz & Cavanaugh, 1995
	6	1	Hügler *et al.*, 2011
Logatchev	6	8	Petersen *et al.*, 2010
	27	9	Guri *et al.*, 2012
Ashadze	4	0	Guri *et al.*, 2012
South MAR	5	5	Petersen *et al.*, 2010
Total	238	68	

| Site | Number of gut clones | | Reference |
	Epsilonproteobacteria	*Gammaproteobacteria*	
Rainbow	6	0	Zbinden & Cambon-Bonavita, 2003
	6	2	Durand *et al.*, 2010
	7	0	*This study*
TAG	1	0	Durand *et al.*, 2010
	0	0	*This study*
Logatchev	6	0	*This study*
Ashadze	7	2	*This study*
Total	33	4	

Figures
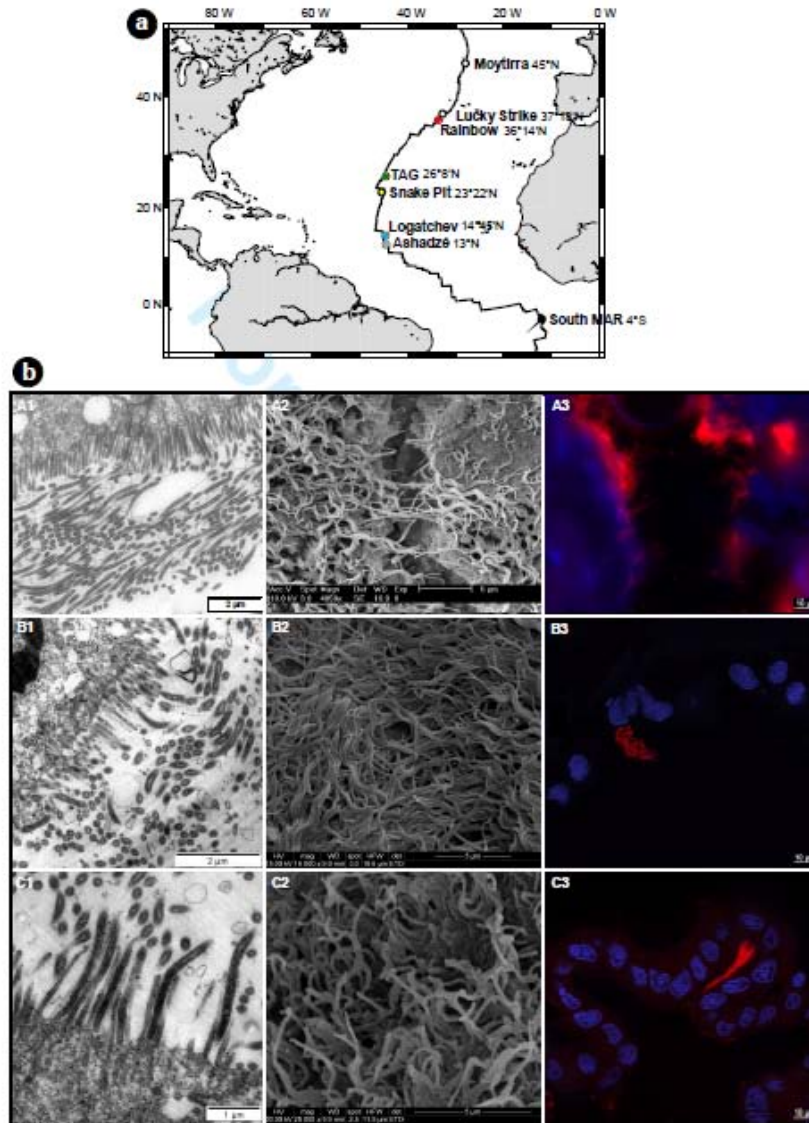
575   **Figure 1** – *R. exoculata* gut epibiont community along the Mid-Atlantic Ridge. **a**, location of the four hydrothermal vent sites studied along the Mid-Atlantic Ridge (modified from Roussel *et al*., 2011). **b**, *R. exoculata* gut filamentous epibionts on Rainbow (A), Logatchev (B) and Ashadze (C) reference specimens observed in transmission electron microscopy (1), scanning electron microscopy (2) and epifluorescence (3). In blue, the shrimp epithelial cells nuclei (DAPI-stained DNA). In red, the filamentous epibionts hybridized with the *Eubacteria*-specific probe Eub338 (Cy3-labelled).

580
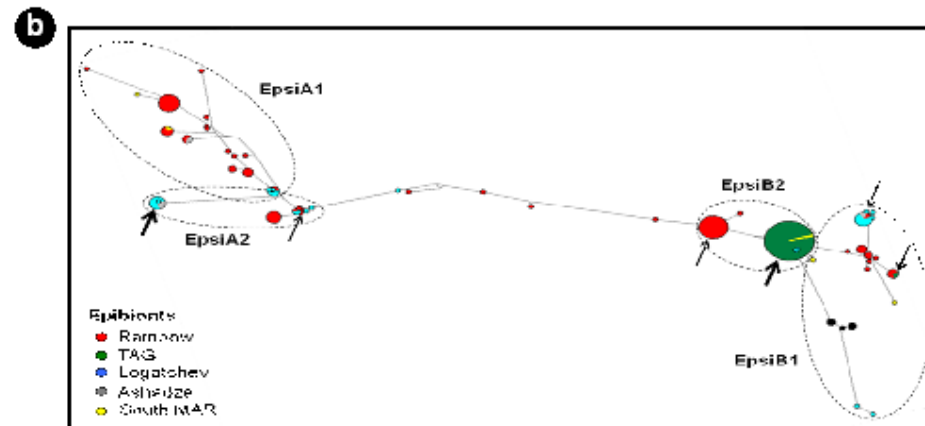
Figure 2 – *R. exoculata* associated *Epsilonproteobacteria* diversity. **a**, *Epsilonproteobacteria* 16S rRNA gene phylogenetic tree calculated on 397 bp, with the neighbor-joining method, the JC model (Jukes & Cantor, 1969) and 1000 bootstraps resampling. Epibionts sequences are labelled as follows: Rainbow gut (R) in red, Rainbow seawater (Rsw) in purple, Rainbow orange chimney (RS1) in orange, Rainbow black chimney (RS2) in light brown, TAG gut (T) in dark green, TAG seawater (Tsw) in turquoise green, TAG black chimney (TS) in light green, Logatchev gut (L) in blue and Ashadze gut (A) in grey. The number of clone sequences is in brackets. The reference gut epibionts sequences

585   are underlined and transcribed rRNA sequences are notified by "td" before the site indication. **b**, network representing 16S rRNA gene evolutionary relationships among the *Epsilonproteobacteria*-related epibionts according to host's site of origin, constructed using the median-joining method applied on 799 bp sequences. Arrows indicate gut ribotype clusters, the larger being in bold.
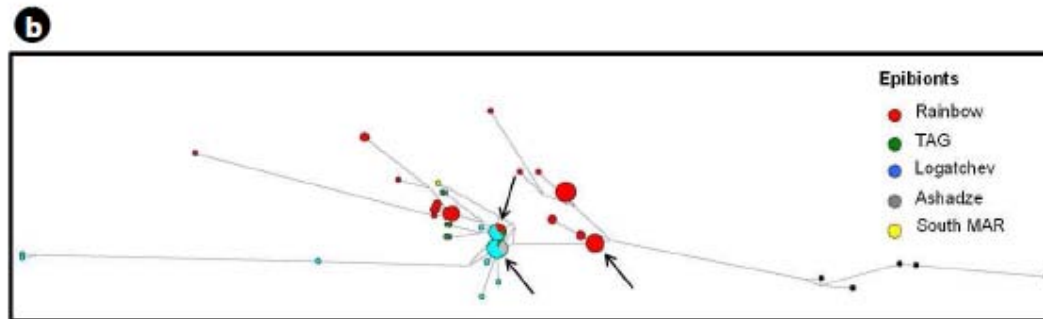
590   **Figure 3** – *R. exoculata* associated *Gammaproteobacteria* diversity. **a**, *Gammaproteobacteria* 16S rRNA gene phylogenetic tree calculated on 639 bp, with the neighbor-joining method, the JC model (Jukes & Cantor, 1969) and 1000 bootstraps resampling. Epibionts sequences are labelled as follows: Rainbow gut (R) in red, Rainbow seawater (Rsw) in purple, Rainbow orange chimney (RS1) in orange, Rainbow black chimney (RS2) in light brown, TAG gut (T) in dark green, TAG seawater (Tsw) in turquoise green, TAG black chimney (TS) in light green, Logatchev gut (L) in blue and Ashadze gut (A) in grey. The number of clone sequences is in brackets. The reference gut epibionts sequences are underlined and transcribed rRNA sequences are notified by "td" before the site indication. **b**, network representing 16S rRNA gene evolutionary relationships among the

595   cluster A of *Gammaproteobacteria*-related epibionts according to host's site of origin, constructed using the median-joining method applied on 884 bp sequences.

Figure 4 – *R. exoculata* associated *Mollicutes* diversity. **a**, *Mollicutes* 16S rRNA gene phylogenetic tree calculated on 762 bp, with the neighbor-joining method, the HKY model

(Hasegawa et al., 1985) and 1000 bootstraps resampling. The tree topology calculated with neighbor-joining or maximum likelihood methods was similar. Epibionts sequences

are labelled as follows: Rainbow gut (R) in red, TAG gut (T) in green and Logatchev gut (L) in blue. The number of clone sequences treated is under the name of the cluster. **b**,

600   network representing 16S rRNA gene evolutionary relationships among the *Mollicutes*-related gut epibionts according to host's site of origin, constructed using the median-

joining method applied on 491 bp sequences (A, 30 clones) and 762 bp sequences (B, 18 clones).
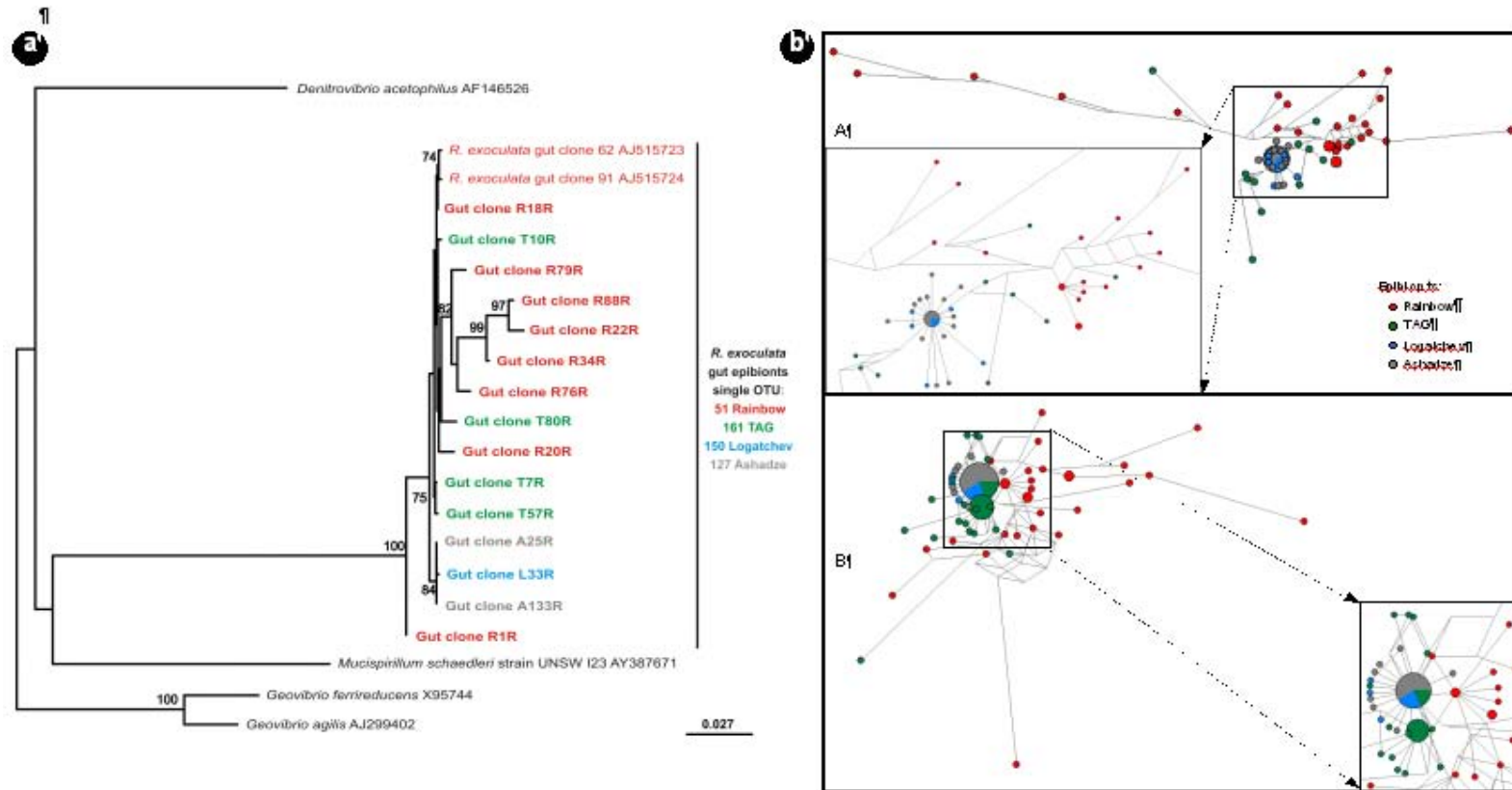
Figure 5 – *R. exoculata* associated *Deferribacteres* diversity. **a**, *Deferribacteres* 16S rRNA gene phylogenetic tree calculated on 696 bp, with the neighbor-joining method, the HKY model (Hasegawa et al., 1985) and 1000 bootstraps resampling. The tree topology calculated with neighbor-joining or maximum likelihood methods was similar. Epibionts sequences are labelled as follows: Rainbow gut (R) in red, TAG gut (T) in green, Logatchev gut (L) in blue and Ashadze gut (A) in grey. The number of clone sequences treated

is under the name of the cluster. **b**, networks representing 16S rRNA gene evolutionary relationships among the *Deferribacteres*-related gut epibionts according to host's site of origin, constructed using the median-joining method applied on 695 bp sequences (A, 69 clones) and 303 bp sequences (B, 96 clones).

Table S1 - Detail of specimens and environmental samples studied per hydrothermal site.

Sites	Samples	DNA	RNA	SEM	TEM	FISH
Rainbow	gut	7	1	3	3	8
	seawater	1	-	-	-	-
	orange chimney RS1	1	-	-	-	-
	black chimney RS2	1	-	-	-	-
TAG	gut	7	1	1	1	2
	seawater	1	-	-	-	-
	black chimney	1	-	-	-	-
Logatchev	gut	6	1	1	2	2
Ashadze	gut	1	1	1	1	1
Total	gut	26	4	6	7	13

Phylogenetic group	Representative clone sequences	First hit of BLAST (accession no.)	Identity (%)	No. of clones*
Deferribacteres	tdR135R, tdR38R, tdR122R, tdR127r, tdA8R, tdA91R, tdA64R, A133R, A076R	Rainbow *R. exoculata* gut clone 91 (AJ515724)	95-99	137 tdR + 4 tdA + 21 A
	R18R, R88R, R22R, R34R, R76R, R20R, R1R	Rainbow *R. exoculata* gut clone R28SW (FM863731)	94-100	51 R + 9 T
	T10R, T80R	TAG *R. exoculata* gut clone T44sul (FM863732)	98-99	19 tdT + 21 tdL + 26 R + 35 T + 12 L
	T7R, T57R, L33R, A25R	TAG *R. exoculata* gut clone T1Fe (FM863733)	99	12 tdT + 13 tdL + 56 T + 73 L + 80 A
	A51R, A65R	Rainbow *R. exoculata* gut clone R49Sul (FM863730)	99	40 tdT + 50 tdL + 61 T + 65 L + 26 A
Mollicutes	tdR168R, tdR93R, tdR175R	Rainbow *R. exoculata* gut clone 42 (AJ515720)	87-99	9 tdR
	tdR106R, T26R, T59R, T31R, tdA25R, tdA62R, tdA6R	Logatchev environmental clone aC4 (FN562893)	97-99	3 tdR + 34 tdA + 41 T + 51 L
	R9R, R19R, R42R	Rainbow *R. exoculata* gut clone R2R (FM881775)	98-99	6 R
	R46R, R38R, R2R	Rainbow *R. exoculata* gut clone R67SW (FM863774)	98	4 R
	T27R, T6R	Rainbow *R. exoculata* gut clone R49LS (FM863736)	99	2 T
	L15xR, tdA57R, tdA59R	Yellow catfish *P. fulvidraco* stomach content clone SC38 (GU293201)	90-94	3 tdA + 4 T + 10 L
	L36R, L41R, L7R, L30R	TAG *R. exoculata* gut clone T8SW (FM863737)	98-99	38 T + 60 L
	tdA46R	Prawn *N. norvegicus* gut clone Se3-204 (GQ866067)	87	3 tdA
Epsilonproteobacteria	tdR132R	Rainbow *R. exoculata* gut clone 88 (AJ515712)	98	3 tdR
	tdR71R	MAR vent organic-rich substrate microcolonizer clone AT-co13 (AY225626)	97-98	8 tdR + 4 T + 7 L
	tdR40R	Iron-mat from submarine volcanoes of Kermadec Arc clone CF-13 (FJ535307)	98	9 tdR
	tdR108R	Vailulu'u Seamount Fe-rich mat/basaltic rocks clone VS_CL-380 (FJ497632)	97	2 tdR
	R28R	Rainbow *R. exoculata* gill chamber epibionts clone LB16S08 (AM902731)	97-99	1 R + 4 L
	R30R, tdA73R, tdA44R	Logatchev *R. exoculata* ectosymbiont clone LOG272/6-9_P2C1 (FM203396)	93-99	3 tdA + 1 R + 2 T + 1 L
	R3R, Rsw-43	Rainbow *R. exoculata* gill chamber epibionts clone LBI7 (AM412509)	98-99	1 R + 1 T + 8 Rsw
	R16R, Rsw-55	Rainbow *R. exoculata* ectosymbiont clone R_c18_eps2 (FM203406)	97-99	1 R + 2 T + 29 Rsw
	R48R	Ventral setae epibiont of *S. crosnieri* hydrothermal crab clone HATO_544 (AB476174)	95	2 R
	T40R, Tsw-5	Snake Pit *R. exoculata* ectosymbiont clone Epsilon S2-16 (FN658696)	97-99	11 T + 9 L + 4 Tsw
	T1360R	Northern Bering Sea sediment clone 090G6 (EU925883)	99	1 T
	L40pR, L10R, L9R, RS1-46	Logatchev environmental clone bH8 (FN562857)	97-98-99	5 L + 4 RS1
	L8xR	Northern Bering Sea sediment clone 090G6 (EU925883)	99	1 L
	L12R	Hydrothermal amphipod *V. sulfuris* tissue clone e34 (FN429840)	98-99	45 L
	L16R	Siliciclastic sediment from Thalassia sea grass bed clone CK_1C4_9 (EU488101)	96	1 L
	L46R	Biofilm at vent orifice of Kermadec Arc clone MS12-1-G08 (AM712341)	95-99	9 T + 4 L
	L11xR	Hydrothermal gastropod *C. squamiferum* clone SF_C23-C6_shell (AY531602)	97-98	3 T + 32 L
	L1423R, L1445R, L1451R, L1347R	Lilliput hydrothermal fluids clone LDGG9 (AM295221)	95-96	1L
	L1409R, L1332R	Pumice fragments exposed to a Mid-Atlantic Ridge vent clone AT-pp13 (AY225610)	96-99	2L
	L1344R	Methane seep sediment clone FeOrig_B_134 (GQ357039)	99	1L
	L1348R	Lost City carbonate chimney clone LC1149b104 (DQ228555)	97	1L

Clone	Closest relative (accession)	%	Distribution
L2325R	Logatchev environmental clone aE8 (FN562833)	98	1 L
L2407R	Amsterdam mud volcano sediment clone AMSMV-5-B33 (HQ588458)	98	1 L
L2419R	Logatchev environmental clone aC8 (FN562859)	99	1 L
L2425R	Hydrothermal worm *Tubificoides benedii* clone 860MI4F#30 (GU197438)	98	1 L
L2488R	Dudley hydrothermal chimney of Juan de Fuca Ridge clone Q1-b39 (FR853051)	97	1 L
L2466R	Oceanic crust clone FS140-2B-02 (AY704396)	96	1 L
A147R, RS1-27, RS1-85	Logatchev environmental clone aF2 (FN562871)	97-99	7 T + 1 A + 2 RS1
A26R	Logatchev *R. exoculata* ectosymbiont clone LOG283/7-4_F1 (FM203395)	99	3 L + 1 A
A021R, Rsw-9	Logatchev fluids clone IIB78 (AM268746)	98	1 L + 9 A + 1 Rsw
A006R	Mothra hydrothermal field (Juan de Fuca Ridge) chimney clone Ba54 (FJ640823)	94-98	7 T + 6 L + 57 A
A61R	Tube of *Lamellibrachia* sp. from cold seep clone V2tb2 (FM165251)	98	9 T + 2 L + 2 A
Rsw-4	Rainbow *R. exoculata* gill chamber epibionts clone LBI26 (AM412516)	98	8 Rsw
Rsw-8	Rainbow *R. exoculata* gill chamber epibionts clone SCAII15 (AM412513)	99	1 T + 2 Rsw
Rsw-60	Rainbow chimney clone ATOS Iris7 Rainbow 26 (AJ969489)	99	2 Rsw
RS1-61	Logatchev environmental clone bC9 (FN562855)	96-99	4 RS1 + 5 T + 1 L
RS1-63	MAR vent organic-rich substrate microcolonizer clone AT-co16 (AY225617)	99	4 RS1
RS1-65, RS2-52, RS2-22	MAR vent clone VC1.2-cl26 (AF367490)	99	1 RS1 + 2 RS2
RS1-33, RS2-74	Logatchev environmental clone aD1 (FN562836)	99	9 RS1 + 6 RS2
RS1-32, RS2-36	Vailulu'u Seamount Fe-rich mat/basaltic rocks clone VS_CL-179 (FJ497628)	98	1 RS1 + 1 RS2
RS1-60	MAR vent clone VC1.2-cl8 (AF367488)	94	1 RS1
RS1-52	Lost City carbonate chimney clone SGYF445 (FJ792210)	93	1 RS1
RS1-51	Lost City carbonate chimney clone SGYF664 (FJ792393)	94	1 RS1
RS1-44	Lake profundal sediment clone c5LKS5 (AM086106)	97	1 RS1
RS1-80, RS1-59	Dudley hydrothermal vent (Juan de Fuca Ridge) clone 4132B5 (EU555136)	94-98	13 RS1
RS1-25	Snake Pit *R. exoculata* ectosymbiont clone Epsilon S1-17 (FN658698)	85	1 RS1
RS1-13	Yellow Sea sediment clone A8S-53 (EU652648)	94	1 RS1
RS2-20	Ventral setae epibiont of *S. crosnieri* hydrothermal crab clone 1208 (AB440163)	97-99	15 T + 2 L + 8 RS2 + 1 RS1
RS2-50	MAR vent iron-rich substrate microcolonizer clone AT-cs3 (AY225614)	99	1 RS2
RS2-72	Logatchev environmental clone aB3 (FN562858)	99	1 tdR + 2 T + 1 RS2
RS2-44	Logatchev environmental clone aH6 (FN562867)	99	1 RS2
RS2-76	Rainbow sulphide sample clone RMB4 (EF644836)	99	1 RS2
RS2-26	Rainbow sulphide sample clone RMB1 (EF644833)	99	1 RS2
RS2-17	Hydrothermal worm *A. pompejana* epibiont *Sulfurospirillum* sp. Am-N (AF357198)	98	1 RS2
RS2-64, RS2-53	*Sulfurimonas autotrophica* DSM16294 from hydrothermal sediment (CP002205)	98	5 RS2
RS2-62	Lost City carbonate chimney clone SGYF599 (FJ792340)	98	1 RS2
RS2-2	Lost City carbonate chimney clone SGXT610 (FJ792021)	95	2 RS2
RS2-77	Rainbow chimney clone PICO pp37 Rainbow 128 (AJ969452)	99	2 RS2
RS2-57, Tsw-79	Iron-mat from submarine volcanoes of Kermadec Arc clone CF-9 (FJ535300)	98-99	2 L + 1 RS2 + 3 Tsw
RS2-92	*Caminibacter mediatlanticus* strain TB-2 (AY691430)	99	1 RS2
Tsw-14	Logatchev environmental clone aH9 (FN562878)	98	2 Tsw
Tsw-20	Juan de Fuca Ridge hydrothermal fluid clone FS396_454_1000bp_0413B (DQ909330)	98	2 Tsw
Tsw-30	*T. benedii* worm from intertidal sediment clone 860MI1G#7 (GU197436)	98	1 L + 7 Tsw
Tsw-67	Vent cap clone VC2.1 Bac1 (AF068783)	98	1 T + 1 Tsw
Tsw-77	Microbial mat from Cesspool Cave clone CC1B_16S_67 (EU662338)	97	1 Tsw
Tsw-73	TAG *R. exoculata* ectosymbiont clone TAG_373_eps171 (FM203385)	98-99	1 tdT + 19 T + 1 L + 4

			Tsw
	Tsw-69	Vent cap clone VC2.1 Bac19 (AF068796)	98	1 Tsw
	TS-23	Guaymas Basin hydrothermal sediment isolate a2b009 (AF420348)	98	1 TS
	TS-5	Suiyo Seamount hydrothermal vent water clone Sd-EB03 (AB193954)	92	1 TS
	TS-16	Dongping Lake sediment clone Shc3-12 (GU208477)	98	1 TS
	TS-12	Symbiotic worm *O. frankpressi* and whale bones clone boneC3F4 (AY548994)	93	1 TS
	TS-35	Cold seep sediment from Gulf of Mexico clone GoM161_Bac1 (AM745129)	95-99	5 T + 2 L + 2 TS
	TS-41	Vailulu'u Seamount Fe-rich mat/basaltic rocks clone VS_CL-14 (FJ497265)	98	1 TS
	TS-40	Deep-sea sediment clone BD2-1 (AB015531)	98	1 T + 3 TS
	TS-37	Vailulu'u Seamount Fe-rich mat/basaltic rocks clone VS_CL-106 (FJ497357)	97	1 TS
	TS-58	Lau Basin active hydrothermal field sediment clone 77 (FJ205272)	95	1 TS
	TS-53	Deep-sea sediment associated with whale falls clone 33mos_0s_H10 (GQ261779)	98-100	6 T + 5 L + 1 TS
	TS-67	Snake Pit *R. exoculata* ectosymbiont clone Epsilon S2-1 (FN658694)	99	2 TS
	TS-90	Pretreatment seawater systems clone SF-July-100 (HM591450)	98	1 TS
	TS-99	Siliciclastic sediment from Thalassia sea grass bed clone CK_1C2_63 (EU487967)	97	2 TS
	TS-85	East Lau Spreading Center hydrothermal sediment clone TGV8BA21 (GQ848422)	98	2 TS
	TS-32, RS2-60	East Lau Spreading Center hydrothermal sediment clone TGV11BA11 (GQ848459)	92-99	1 TS + 1 RS2
	TS-11	Iron-oxidizing mat from Chefren mud volcano clone 102B123 (EF687160)	89	1 TS
	Tsw-37	Ventral setae epibiont of *S. crosnieri* hydrothermal crab clone HAT3_417 (AB476195)	96	1 Tsw
Gammaproteobacteria	R12R	Rainbow *R. exoculata* ectosymbiont clone R_c20_gam1 (FM203378)	99	1 R + 3 Rsw
	R26R	Rainbow *R. exoculata* ectosymbiont clone R_c18_B9 (FN393021)	99	3 R
	tdA5R	Logatchev *R. exoculata* ectosymbiont clone LOG_272/6-9_A1 (FN393025)	96-99	3 tdA + 1 T + 4 L
	tdA82R	Bovine rumen content clone L102RC-4-G11 (HQ399822)	95	3 tdA
	L2321R	Environmental clone C02 (AB597540)	89	1 L
	L1461R	*Photobacterium* sp. NF1-15 (FJ889641)	94	1 L
	L1466R	*Photobacterium leiognathi* strain SN2B (AY292951)	96	1 L
	Rsw-70, Rsw-85	Rainbow *R. exoculata* gill chamber epibionts clone SC16S36 (AM902727)	97-99	2 L + 2 Rsw
	RS1-6, RS2-41	Haakon Mosby mud volcano sediment clone HMMVCen-4 (AJ704661)	99	1 RS1 + 1 RS2
	RS1-5, RS1-94	Logatchev *B. puteoserpentis* methanotrophic endosymbiont clone pLOG-2-6 (AM083965)	97-99	2 RS1
	RS1-10	Arctic Ocean water clone Arctic96AD-9 (AF354608)	94	1 RS1
	RS1-45, RS1-53, Tsw-65	Deep-sea water from hydrothermal vent area clone SSmCB09-52 (AB176166)	98-99	19 RS1 + 2 Tsw
	RS1-24	Logatchev sulphide sample clone L8B10 (EF644812)	98	1 RS1
	RS1-50	Logatchev sulphide sample clone L7B5 (EF644791)	93	1 RS1
	RS1-90	Yellow Sea sediment clone A13S-75 (EU617815)	96	1 RS1
	RS2-16, RS2-85	*Colwellia piezophila* strain Y223G from deep-sea sediment (NR_024805)	98	2 RS2
	RS2-8	Donana coastal aquifer clone 49S1_1B_55 (DQ837294)	99	1 RS2
	RS2-19, RS2-70, RS2-99, Tsw-50	*Escherichi coli* KO11 (CP002516)	99	5 RS2 + 1 Tsw
	RS2-37	*Serratia* sp. 136-2 from soil (EU557341)	99	1 RS2
	RS2-34	Deep seawater from the EPR clone EPR4055-N3-Bc63 (EU491928)	98	1 RS2
	RS2-49	*H. sapiens* skin clone ncd112e08c1 (JF011316)	99	1 RS2
	RS2-46	*Salmonella enterica* strain T000240 (AP011957)	99	1 RS2
	RS2-63	Hair of hydrothermal crab *S. crosnieri* epibiont *Leucothrix* sp. clone B16 (EU107481)	98	3 RS2
	RS2-75	Blue mud wasp *C. californicum* abdomen clone SHNU448 (HM110455)	99	1 RS2
	Tsw-36	Soil aggregate clone BacA_064 (EU335291)	99	1 Tsw
	Tsw-17	*Marinobacter hydrocarbonoclasticus* isolate OC-11 from tropical marine sediment (AY669171)	99	1 Tsw

	Tsw-9	Wadden Sea intertidal sediment clone JSS S04 317 (HQ191049)	91	1 Tsw
	Tsw-40	Enriched seawater polluted by Tunisian crude oil uncultured bacterium (CU915011)	96	1 Tsw
	Tsw-49	Seawater clone 6S232425 (EU804489)	99	1 Tsw
	Tsw-47, TS-87	Vailulu'u Seamount Fe-rich mat/basaltic rocks clone VS_CL-357 (FJ497609)	98	1 Tsw + 1 TS
	Tsw-56	*Shigella boydii* strain GTC779 (AB273731)	99	1 Tsw
	Tsw-82	TAG *R. exoculata* ectosymbiont clone TAG_366_gam5 (FM203381)	98-99	1 T + 20 Tsw
	Tsw-76	Elephant *L. africanus* feces clone AFEL3_aao16a10 (EU466025)	99	1 Tsw
	Tsw-85	Lost City carbonate chimney clone SGYF471 (FJ792231)	99	1 Tsw
	Tsw-90, TS19	Mothra hydrothermal field (Juan de Fuca Ridge) chimney clone Ba2 (FJ640843)	98	1 T + 1 Tsw + 1 TS
	Tsw-19	Mothra hydrothermal field (Juan de Fuca Ridge) chimney clone Ba8 (FJ640811)	90	1 Tsw
	Tsw-96	Red panda feces clone RP_1aaa01e08 (EU778504)	99	4 TS
	TS-29	Ventral setae epibiont of *S. crosnieri* hydrothermal crab clone IHEO_1109 (AB476230)	97	1 TS
	TS-22	Ventral setae epibiont of *S. crosnieri* hydrothermal crab clone HATO_655 (AB476182)	98	2 TS
	TS-51, TS-38	Logatchev sulphide sample clone L7B4 (EF644790)	95-99	29 TS
	TS-82	Marine sediment (Cascadia Margin) above gas hydrate ridge clone Hyd24-01 (AJ535221)	95	1 TS
	TS-57	Ventral setae epibiont of *S. crosnieri* hydrothermal crab clone IHEO_1064 (AB476225)	95	1 TS
Alphaproteobacteria	T2323R	Deep sea octocoral clone ctg_CGOF223 (DQ395681)	98	1 T
	RS1-86, RS1-57, RS1-35, RS2-10, Tsw-16, TS-62, TS-72, TS-76	Marine hydrocarbon seep sediment clone Ethane SIP4-6-06 (GU584499)	96-99	4 RS1 + 1 RS2 + 1 Tsw + 5 TS
	T192R, T2429R	Lost City carbonate chimney clone LC1133B-90 (DQ270648)	97	2 T
	RS1-8	TAG black smoker chimney clone TI_chim_Sur55-1 (AB518773)	99	1 RS1
	RS2-24, RS2-32	Logatchev environmental clone bB10 (FN562825)	99	3 RS2
	RS2-58	Biofilm clone ZBAF3-8 (HQ682047)	94	1 RS2
	RS2-67	Hydrothermal vent chimney of Guaymas Basin clone 21B42 (DQ925896)	98	1 RS2
	RS2-81	White biofilm on shallow hydrothermal vent of South Tonga Arc clone V1B07b191 (HQ153899)	98	2 RS2
	RS2-98	Vailulu'u Seamount Fe-rich mat/basaltic rocks clone VS_CL-289 (FJ497541)	98	1 RS2
	Tsw-52	Hydrothermal amphipod *V. sulfuris* tissue clone i32 (FN429823)	99	1 Tsw
	Tsw-70	Deep oxygen minimum zone of Northeast subarctic Pacific Ocean clone F9P261000_S_O01 (HQ674273)	99	1 Tsw
	Tsw-71	Deep Northeast subarctic Pacific Ocean clone F9P262000_S_A19 (HQ674323)	99	1 Tsw
	Tsw-32	*Rickettsia* from deep ocean water (6000m depth) from Puerto Rico Trench clone PRTAB7729 (HM798661)	98	1 Tsw
	TS-20	Gulf of Mexico clone 230-15-2 (HQ433399)	98	1 TS
	TS-43, TS-14	Deep seawater from the EPR clone EPR4055-N3-Bc35 (EU491911)	93-99	2 TS
	TS-6	Logatchev sulphide sample clone L8B4 (EF644806)	99	1 TS
	TS-31	Symbiont of deep-sea hydrothermal polychaete from Okinawa Trough clone HPf-28 (AB244979)	99	2 Ts
	TS-45	Amsterdam mud volcano sediment clone AMSMV-0-B116 (HQ588399)	99	1 TS
	TS-52	Deep marine hydrothermal sediment from Lau Basin clone I2A (FJ205314)	98	1 TS
	TS-79	Kazan mud volcano clone KZNMV-5-B16 (FJ712457)	93	1 TS
	TS-86	Kazan mud volcano clone KZNMV-10-B51 (FJ712530)	90	1 TS
	TS-84	Arctic surface sediment clone B78-13 (EU286977)	90	1 TS
	TS-88	Coastal water biome from a Norway fjord clone 16_06_03F06 (FR683520)	90	1 TS
	TS-95	Lost City carbonate chimney clone LC1133B-74 (DQ270646)	99	1 TS
Betaproteobacteria	tdA95R	Biofilm of extubated tracheal tube clone ET_B_4b02 (FJ557277)	99	1 tdA
	tdA26R	Aquifer sediment clone RABS_B98 (HQ660905)	99	1 tdA
	RS2-87, RS2-51	Carpet-like mucilaginous cyanobacterial blooms in hypereutrophic lake clone E161 (HQ828049)	99	2 RS2

	RS2-12, RS2-40	*H. sapiens* skin, antecubital fossa clone ncd1276c11c1 (FJ107333)	98-99	2 RS2
	RS2-43	*H. sapiens* skin, popliteal fossa clone ncd905g08c1 (FJ082186)	98-99	1 T + 1 RS2
	RS2-54	Butterfly *R. lebeau* egg clone 298EGG26 (FJ593728)	99	1 RS2
	Tsw-97, Tsw-92	Leafcutter ant *A. columbica* colony N12 fungus garden bottom clone BICP1477 (HM557329)	95	2 Tsw
	Tsw-27	*Ralstonia* sp. from Red Sea Atlantis II deep-sea brine water clone Atlantis II_d (HQ530524)	99	2 Tsw
Deltaproteobacteria	tdR182R, Rsw-42	Snake Pit *R. exoculata* ectosymbiont clone Delta S1-6 (FN658700)	98	1 tdR + 1 Rsw
	L37R, tdA23R, tdA30R, tdA56R, tdA71R, tdA66R	Logatchev hydrothermal fluids clone IIB75 (AM268749)	99	8 tdA + 3 L
	L37R	Wadden Sea surface sediment clone SB14 (AY771938)	94	1 L
	L2475R	Logatchev hydrothermal fluids clone IIB152 (AM268749)	97	1 L
	tdA28R, tdA50R	Logatchev hydrothermal fluids clone IIB133 (AM268767)	98-99	2 tdA + 2 L
	RS1-75	*Desulfothermus okinawensis* (AB264617)	95	1 RS1
	RS2-61, RS2-66, RS2-73, RS2-84	Rainbwow sulphide sample clone ROB7 (EF644847)	99	8 RS2
	Tsw-33	Hydrothermal vestimentiferan *R. pachyptila* tube R103-B13 (AF449229)	99	1 Tsw
	Tsw-42	Oceanic dead zone (Saanich Inlet, 100m depth) clone SGST650 (GQ348094)	97	1 Tsw
	Tsw-19	Deep ocean water (6000m depth) from Puerto Rico Trench clone PRTBB8646(HM799049)	99	1 Tsw
	TS-83	Rainbow chimney clone PICO pp37 Rainbow 32 (AF449228)	92	1 TS
	TS-93	Hydrothermal vestimentiferan *R. pachyptila* tube R103-B27 (AF449228)	91	1 L + 1 TS
Zetaproteobacteria	T1481R	TAG *R. exoculata* gut clone T10Sul (FM863751)	97	1 T
	RS2-71	Hydrothermal mat from Lohiau Vent at Loihi clone Loh_60 (FJ001796)	93	1 RS2
	RS2-95,Tsw-13, Tsw-74	Deep hydrothermal fluid from Mariana Trough clone Papm3BL54 (AB284833)	98	1 RS2 + 2 Tsw
CFB	tdR63R	Microbial mat from Cesspool Cave clone CC1_16S_16 (EU662369)	93	5 tdR
	R14R	Uncultured *Bacteroidetes* from estuarine sediment clone C139a-R8C-D4 (AY678514)	95	2 R
	T70R	Hydrothermal sediment from Southern Okinawa Trough clone p816_b_3.23 (AB305587)	92	1 T
	T2469R	Northeast subarctic Pacific Ocean clone F9P2610_S_L10 (HQ672162)	89	1T
	T2467R	South MAR *R. exoculata* ectosymbiont clone SM146623_148 (FN662612)	99	1T
	tdA15R	Hydrothermal worm *P. palmiformis* mucus secretion clone P. palm A 10 (AJ441240)	98	1 tdA
	L195R	Hydrothermal gastropod clone C11-F10 (AY355298)	98	1 L
	L2362R	South MAR *R. exoculata* ectosymbiont clone SM146623_153 (FN662606)	98	1L
	Rsw-79	Snake Pit *R. exoculata* ectosymbiont clone Bacteroidetes S2-2 (FN658702)	99	4 Rsw
	RS1-21	Yellow Sea intertidal seawater clone 5m-27 (GU261224)	98	2 RS1
	RS1-73	Gulf of Mexico active mud volcano GoM GB425 68B-43 (AY542563)	96	1 T + 1 RS1
	RS1-62, TS-2	Arctic Ocean water clone b72 (EU919789)	98	2 RS1 + 1 TS
	RS2-21	Raw seawater clone SW-Apr-83 (HQ203953)	98	1 RS2
	RS2-100, RS2-91, TS-63, TS-15	Tube of *Lamellibrachia* sp. from cold seep clone V2tb8 (FM165250)	94-99	1 L + 2 RS2 + 2 TS
	Tsw-87	Iron-oxide chimney-like structure from Tonga Arc clone V19F55b (FJ905651)	93	1 Tsw
	Tsw-45	Northeast subarctic Pacific Ocean clone F9P26500_S_P20 (HQ673054)	98	1 Tsw
	Tsw-23	Sulphide chimney from Juan de Fuca Ridge clone PS-B23 (AY280420)	95	1 Tsw
	Tsw-24	Cytophaga sp. isolate BHI80-3 (AJ431238)	99	1 Tsw
	TS-49	Logatchev chimney clone bA10 (FN562914)	98	1 TS
	TS-46	Marine reef sandy sediment clone AO4 (FJ358900)	95	1 TS
Verrucomicrobiae	T41R, T20R, T29R	Tube of *Lamellibrachia* sp. from cold seep clone V1t43 (FM165269)	95-98	3 T

	T43R	Sandy carbonate sediment clone CI75cm.2.89 (EF208729)	94	1 T
	T72R	Active hydrothermal chimney from Okinawa Trough clone HTM871W-B43 (AB611176)	92	1 T
	T179R	Particulate detritus associated with *Ridgea piscesae* clone HF8GH2b42 (JN662163)	98	1 T
	L45R	Microfiltration system clone MF-Jan-42 (HQ225122)	98	2 L
	TS-91	Northern Bering Sea surface water clone s30 (GQ452875)	92	1 TS
Firmicutes	R8R	TAG *R. exoculata* gut clone T28SW (FM863738)	99	1 R + 3 T
	T17R	Butterfly *S. littoralis* gut uncultured *Clostridium* clone SL29 (HQ264089)	89-90	7 tdT + 32 T
	RS2-47	Uncultured *Staphylococcus* sp. from spacecraft associated clean room clone JPL-S3_I17 (FJ957639)	95	1 RS2
	T1417R, T2379R	TAG *R. exoculata* gut clone T17SW (FM863763)	98	2 T
	tdT122R, tdT130R , T1426R, T1438R, T1440R, T1447R, T1453R, T1463R, T1489R, T1493R, T124R, T164R, T165R, T168R, T172R, T173R, T177R, T196R	Clostridiaceae clone SHO21 from resuspended plant residue in a methanogenic reactor (AB298756)	90-92	2 tdT + 24 T
Actinobacteracea	tdA41R, tdA90R	Indoor dust clone BF0002A028 (AM696843)	99	2 tdA
	L138R, L161R	Activated sludge from batch reactor clone 0-4-24 (JN609310)	92-94	2 L
Thermodesulfobacteracea	RS1-66, RS1-68	Rainbow chimney *Thermodesulfobacterium* clone PICO pp37 Rainbow 201 (AJ969460)	93-99	2 RS1
	RS1-91, RS2-48	Rainbow chimney *Thermodesulfatator* sp. clone AT 1325 (EU435435)	99	1 RS1 + 1 RS2
Aquificales	RS1-49, RS2-59	Rainbow chimney *Aquificales* clone PICO pp37 Rainbow 28 (AJ969464)	96-99	1 RS1 + 1 RS2
	RS2-94	Rainbow chimney *Aquificales* clone PICO pp37 Rainbow 62 (AJ969466)	99	1 RS2
Chloroflexi	T2430R	TAG chimney clone pMARB10_31 (AB496522)	97	1 T
Unaffiliated	tdA43R, tdA83R	Hydrothermal yeti crab *K. hirsuta* epibiont clone F8 (EU265798)	96	2 tdA
	L2323R	Yonaguni Knoll IV hydrothermal chimney clone pYK04-20B-13 (AB464836)	97	1 L
	L1427R	Hydrothermal fluids from Juan de Fuca Ridge clone FS312_454_1000bp_0842B (DQ910026)	95	1 L
	RS1-95, RS1-76	Hydrothermal worm *P. palmiformis* mucus secretion clone P. palm C72 (AJ441233)	87-88	2 RS1
	Tsw-72, Tsw-35	Deep-sea hydrothermal vent clone aH11 (FN562888)	87-97	1 L + 2 Tsw
	Tsw-83	Deep seawater (6000m depth) from Puerto Rico Trench clone PRTAB7827 (HM798723)	99	1 Tsw
	T1479R	Hydrothermal sediment clone p760_b_3.29 (AB305412)	91	1 T

Figure S1 – Mid-Atlantic Ridge hydrothermal sites. Sampling location of the four hydrothermal sites studied: (a) Rainbow, (b) Ashadze, (c) TAG, (d) Logatchev general view and (e) Logatchev Irina II vent detailed view showing the shrimps location just beside the mussel bed. A = anemone, M = mussels, S = shrimps and V = vent.
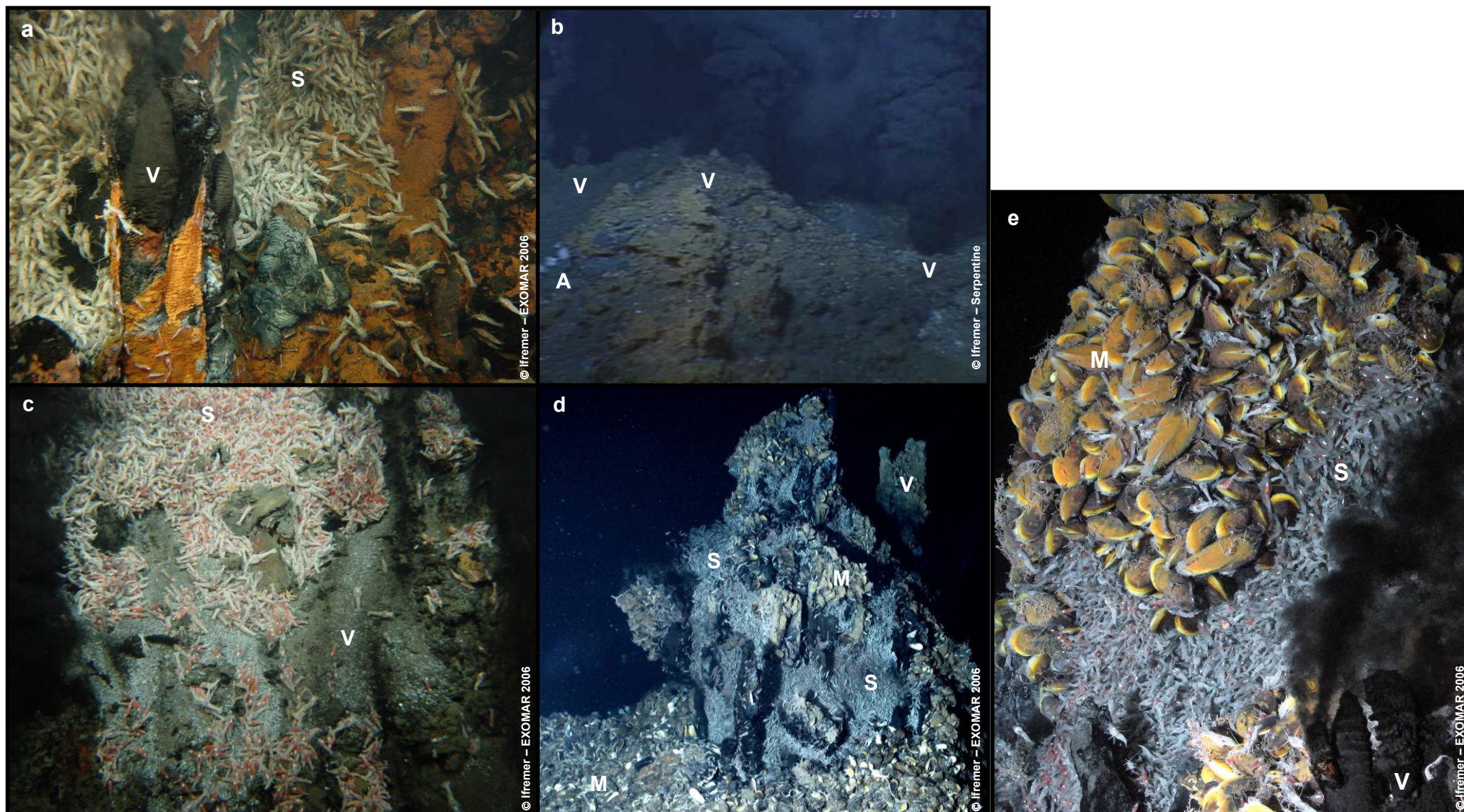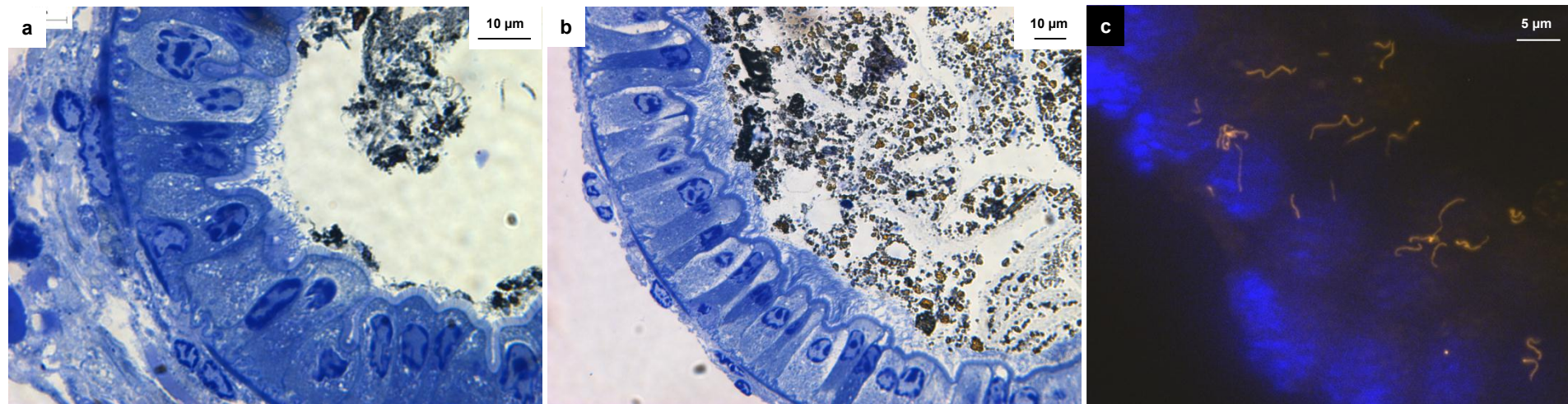
Figure S2 – *Rimicaris exoculata* gut filamentous epibionts in juvenile specimens from Rainbow. *Light microscopy observations*: **a,** juvenile total lenght was 2.25 cm and **b,** juvenile total lenght was 3 cm. *Epifluorescence observation* (fluorescence *in situ* hybridization): **c,** juvenile total lenght was 1.6 cm, in blue the DAPI-labelled nuclei of the shrimp gut epithelium, and in red the epibionts hybridized using the Cy3-labelled Eub338 probe.
Shrimp collection and selection. Juvenile specimens of *R. exoculata* were collected during the French MOMAR 08 cruise at the Rainbow vent site. The gut samples were fixed and observed as described in Durand *et al.*, 2010.

Figure S3 – Location and structure of Rainbow hydrothermal site. **A**, Mid-Atlantic Ridge Azorean segment topology showing the Rainbow site, protected by the Azorean plateau, and distant from the three other sites studied (TAG, Logatchev and Ashadze). **B**, relief representation of Rainbow site surroundings. Green triangles represent ultramafic-hosted sites and red one represents basalt-hosted site.